AD_____

Award Number: DAMD17-99-1-9541

TITLE: Neuronal Degeneration in the Cingulate Gyrus: NMDA Antagonists and Anticholinesterases

PRINCIPAL INVESTIGATOR: Wilkie A. Wilson, Ph.D.

CONTRACTING ORGANIZATION: Duke University Medical Center
Durham, North Carolina 27710

REPORT DATE: October 2000

TYPE OF REPORT: Annual

PREPARED FOR: U.S. Army Medical Research and Materiel Command
Fort Detrick, Maryland 21702-5012

REPORT DOCUMENTATION PAGE

Form Approved
OMB No. 074-0188

1. AGENCY USE ONLY (Leave blank)	2. REPORT DATE	3. REPORT TYPE AND DATES COVERED
	October 2000	Annual (30 Sep 99 – 29 Sep 00)

4. TITLE AND SUBTITLE
Neuronal Degeneration in the Cingulate Gyrus: NMDA Antagonists and Anticholinesterases

5. FUNDING NUMBERS
DAMD17-99-1-9541

6. AUTHOR(S)
Wilkie A. Wilson, Ph.D.

7. PERFORMING ORGANIZATION NAME(S) AND ADDRESS(ES)
Duke University Medical Center
Durham, North Carolina 27710

E-MAIL: wawilson@acpub.duke.edu

8. PERFORMING ORGANIZATION REPORT NUMBER

9. SPONSORING / MONITORING AGENCY NAME(S) AND ADDRESS(ES)
U.S. Army Medical Research and Materiel Command
Fort Detrick, Maryland 21702-5012

10. SPONSORING / MONITORING AGENCY REPORT NUMBER

11. SUPPLEMENTARY NOTES
Report contains color graphics.

12a. DISTRIBUTION / AVAILABILITY STATEMENT
Approved for public release; Distribution unlimited

12b. DISTRIBUTION CODE

13. ABSTRACT *(Maximum 200 Words)*

The goal of this study is to understand the interaction between drugs that are antagonists at the NMDA receptor subtype of glutamate receptors and drugs that are anticholinesterases. Previous research showed that NMDA antagonists are neurotoxic in the cingulate/retrosplenial cortex and that this toxicity was enhanced by muscarinic cholinergic agonists. We hypothesized that anticholinesterases would also enhance the toxicity of these compounds. We have used three approaches in this study: 1) We used intracellular electrophysiology; 2) We used imaging of brain slices treated with voltage sensitive dyes; 3) We used a stain (Fluro-Jade) which identifies dying neurons. Each of these approaches showed that NMDA antagonism produces excitability and/or neurotoxicity in these brain areas. Surprisingly, the anticholinesterase pyridostigmine appears to be inhibitory and preliminary studies suggest that it may protect against NMDA antagonist neurotoxicity. Our second year of experiments will continue this line of research.

14. SUBJECT TERMS	15. NUMBER OF PAGES
Neurotoxin	89
	16. PRICE CODE

17. SECURITY CLASSIFICATION OF REPORT	18. SECURITY CLASSIFICATION OF THIS PAGE	19. SECURITY CLASSIFICATION OF ABSTRACT	20. LIMITATION OF ABSTRACT
Unclassified	Unclassified	Unclassified	Unlimited

NSN 7540-01-280-5500

Standard Form 298 (Rev. 2-89)
Prescribed by ANSI Std. Z39-18
298-102

TABLE OF CONTENTS

Introduction

The key objectives of these studies are to determine the neurotoxic risks of combining inhibitors of acetylcholinesterase (AChE) enzymes and blockers of N-methyl-D-aspartate receptor or channels (NMDAr/c). As more drugs are being developed that are NMDAr/c antagonists, therapeutic combinations are likely to occur in military or civilian settings. For example, these may be used in combination to prevent toxicity from chemical warfare that act on AChE enzymes (e.g., soman), or to treat symptoms of exposure to these agents. There are three approaches with which we are attacking these objectives:

1. We have used electrophysiological studies, including patch clamp recordings of single neurons, to test the hypotheses proposed regarding the mechanisms by which NMDA r/c antagonist-mediated toxicity occurs. We used rat brain slices that include posterior cingulate/retrosplenial cortecies (PC/RSC) and parietal cortex to test the hypothesis that MK-801 produces neurotoxicity by disrupting GABAergic inhibition, and that this disruption is greater in the PC/RSC than other cortical areas. Our results are consistent with these hypotheses. Specifically, it has been hypothesized that a decrease in excitatory drive to interneurons caused by NMDA antagonists could result in disinhibition of principal cells and, in turn, this disinhibition (and resulting hyperexcitability) might be responsible for neurotoxicity or neurodegeneration.

We examined the effects of the NMDA receptor antagonist, MK-801, on $GABA_A$-mediated inhibitory post-synaptic currents (IPSCs) of pyramidal neurons in the retorsplenial cortex (RSC), an area showing a great sensitivity to MK-801-induced neuronal death. Using whole-cell patch clamp techniques, bicuculline-sensitive IPSCs were isolated and recorded from biocytin-labeled pyramidal neurons in the RSC and parietal cortex of young rats. Bath application of MK-801 (10-40μM) caused a concentration-dependent decrease in frequency of spontaneous IPSCs in the majority of recorded pyramidal cells; MK-801 also reduced the amplitude of evoked $GABA_A$ receptor-mediated IPSCs in pyramidal neurons recorded in layer II-VI. When compared to pyramidal neurons in the parietal cortex, MK-801 showed a greater inhibitory effect on IPSCs in the RSC. This finding, too, is consistent with the proposed hypothesis regarding anatomical vulnerabilities.

2. Photodiode images of voltage-sensitive dye-treated slices were used to assess acute changes across cell layers in the posterior cingulate/retrosplenial cortecies to test possible neurotoxic combinations. Preliminary findings suggest that MK-801 at a low concentration (3μM) causes depolarization in brain slices from adult rats that include the posterior cingulate gyrus or retrosplenial cortex, whereas pyridostigmine (100μM) is inhibitory.

3. Histological measures were used to assess neurotoxicity after *in vivo* exposure to drug combinations. The most successful histological method we used was the new stain, Fluoro-Jade. In preliminary studies, we have found that MK-801 (0.3-3 mg/kg, s.c.) produces neurodegeneration in the posterior cingulate gyrus and retrosplenial cortex. Given alone, pyridostigmine bromide (PB) (0.1 mg/kg) produces no neurodegeneration. Given in combination with MK-801, PB does not appear to produce gross enhancement of the neurodegeneration caused by MK-801 (0.3 mg/kg). (In several animals, PB appeared to be slightly protective; however, the responses were quite variable, and more animals, different doses, and different orders of administration must be tested to rule out windows of synergistic neurotoxicity.)

Body

During this reporting period the following studies have been carried out:

A. MK-801, an NMDA Receptor Antagonist, Modulates the Inhibitory Postsynaptic Currents (IPSCs) in Pyramidal Neurons in the Rat Cingulate and Retrosplenial Cortecies.

B. Using Voltage Sensitive Dyes to Image the Effect of an NMDA Antagonist and Pyridostigmine in the Rat Cingulate Gyrus and Retrosplenial Cortex

C. Using Fluoro-Jade Staining to Measure Interactions between NMDA Antagonists and Acetylcholinesterase Inhibitors in the Rat Cingulate Gyrus and Retrosplenial Cortex

MK-801, AN NMDA RECEPTOR ANTAGONIST, MODULATES THE INHIBITORY POSTSYNAPTIC CURRENTS (IPSCs) IN PYRAMIDAL NEURONS IN THE RAT CINGULATE /RETROSPLENIAL CORTICES

Qiang Li, Suzanne Clark, Darrell V. Lewis and Wilkie A. Wilson

Department of Pharmacology and Cancer Biology and Pediatrics (Neurology), Duke University Medical center. Neurology Research, Veterans Administration Medical Center, Durham, NC, 27705

Keywords: MK-801, NMDA receptor, IPSCs, Pyramidal cells, Interneurons, Cingulate gyrus, RSC.

Address correspondence to:

Qiang Li, MD.,Ph.D

Neurology Research

Room 21, Building 16 VAMC

508 Fulton Street, Durham, NC 27705

Fax: 919-286-4662

E-mail:Liq@duke.edu

Running title: MK-801 and IPSCs of cortical pyramidal cells

Abstract

A decrease in the excitatory drive to interneurons caused by *N*-methyl-D-aspartate (NMDA) antagonists could cause disinhibition of the principal cells and, in turn, this disinhibition (resulting in hyperexcitation) might be responsible for neurotoxicity or neuronal degeneration. In the present study, we examined the effects of the NMDA receptor antagonist, MK-801, on $GABA_A$-mediated inhibitory post-synaptic currents (IPSCs) of pyramidal neurons in the retrosplenial cortex (RSC). Using whole-cell patch clamp techniques, bicuculline-sensitive IPSCs were isolated and recorded from biocytin-labeled pyramidal neurons in the RSC and parietal cortex of rats (P14-25). At the holding potential of -5 to +30 mV, bath application of MK-801 (10-40μM) caused a dose-dependent decrease in frequency of spontaneous IPSCs in the majority of recorded pyramidal cells; MK-801 also reduced the amplitude of evoked $GABA_A$ receptor-mediated IPSCs in pyramidal neurons. When compared to pyramidal neurons in the parietal cortex, MK-801 showed a greater inhibitory effect on IPSCs in the RSC. In the presence of 0.5 μM tetrodotoxin (TTX), the amplitude and frequency of the miniature IPSCs (mIPSCs) were not affected by bath application of MK-801 (40μM). The present results suggest that NMDA receptors regulate spontaneous activity of inhibitory interneurons and thereby GABA release in specific cortical areas. Therefore blockade of NMDA receptors causes a region-specific decrease in inhibitory input to pyramidal cells. This effect may explain in part the regional neurotoxicity of NMDA receptor antagonists.

Introduction

Excessive release of glutamate with subsequent over-activation of N-methyl-D-aspartate (NMDA) receptors is thought to be responsible for neuronal injury or damage under certain pathological conditions (Rothman and Olney 1986, 1987). Accordingly, in an attempt to attenuate glutamate-mediated neurotoxicity, several NMDA receptor antagonists have been tried in a range of animal models and clinical trials including epilepsy (Avoli and Olivier 1987) and ischemia (Aitken et al, 1988, Ford et al, 1989, Rod and Auer, 1989). Among selective NMDA antagonists, MK-801 (dizocilpine-maleate), a non-comparative NMDA channel blocker, has been widely used to investigate the involvement of NMDA receptors in these pathological conditions and has shown some beneficial effects in animal models by preventing or reducing neuronal injury and damage. However, in clinical trials, some NMDA antagonists produced unpleasant side effects that significantly limited their tolerability in humans. The mechanism of these side effects is not completely understood but one possible mechanism has been described by Olney and his colleagues who discovered that certain NMDA antagonists caused neurotoxicity in selected areas of the rat brain. (Olney et al 1989, 1991).

As one important limbic component of the mammalian brain, the cingulate cortex is a key area implicated in emotion and many neuropsychiatric disorders (Cummings, 1993). In addition, the cingulate and retrospleninal cortex (RSC) of rats are selectively susceptible to the toxic effects of MK-801, compared with other brain areas examined (Olney et al, 1990, Allen and Iversen, 1990, Horvath et al, 1997). The pathomorphological changes in rats treated with MK-801 varied from dilation of mitochondria and endoplasmic

reticulum at low doses and to neuronal death in high doses (Olney et al 1989, Fix et al 1995, Olney et al 1991, Horvath et al, 1997). Based on these surprising findings, Olney et al (1995) hypothesized that prolonged inactivation of NMDA receptor function by NMDA antagonists, such as MK-801, phencyclidine (PCP) and ketamine, resulted in NMDA receptor hypofunction, which disrupted the balance between excitation and inhibition and led to excitotoxic neuronal injury in selected brain regions including the RSC (Grunze et al, 1996).

Although evidence derived from a number of in vivo studies have supported the NMDA receptor antagonist induced disinhibition hypothesis originally proposed by Olney et al (1991), a direct in vitro test of this hypothesis has not been done yet. In the present study, we utilized whole-cell patch clamp recording techniques and examined the effects of the NMDA receptor antagonist, MK-801, on the $GABA_A$ receptor-mediated IPSCs of pyramidal neurons in the RSC. We provided a direct electrophysiological evidence, for the first time, that blockade of NMDA receptors by MK-801 caused a decrease in inhibitory synaptic drive to pyramidal cells in the RSC. In addition, there are also regional differences in this effect that may help explain specific anatomical vulnerabilities. Some preliminary results of the present work have been published in abstract form (Li et al, 2000).

Materials and Methods

Cortical slices

Cortical slices were prepared from young, male Sprague-Dawley rats (P15-P25). Rats were iosflurane-anesthetized and decapitated. The brains were quickly removed from the skulls and placed in a cold (4°C) artificial cerebrospinal fluid (ACSF) containing (in mM) 120 NaCl, 3.3 KCl, 1.23 NaH_2PO_4, 1.2 $MgSO_4$, 1.8 $CaCl_2$ and 10 D-Glucose at pH 7.3, previously saturated with 95%O_2/5%CO_2. Coronal cortical slices containing retrosplenial granule cortex (RSC) (Paxinos and Watson, 1986) (300μm thickness) were cut with a vibratome (Campden, Model 752, England) and incubated in a holding chamber continuously bubbled with 95% O_2/5% CO_2 at room temperature (20-24°C).

Whole Cell Voltage-clamp recording

Our whole-cell patch clamp techniques have been described in our previous publication (Mott et al, 1999). For recording, patch pipettes were pulled from borosillicate glass capillary tubing (1.5mm O.D., 1.05 mm I.D., World Precision Instrument, Sarasota, FL) on a Flaming-Brown horizontal microelectrode puller (Model P-87, Sutter Instrument Co, Novato, CA). Pipettes were filled with an intracellular solution containing (in mM) 130 Cs-Gluconate, 7 CsCl, *10 N-2-hydroxyethylpiperazine-N,N,N',N'-tetraacetic acid* (HEEPS), 4 Mg-ATP (pH=7.25). The quaternary lidocaine derivative QX-314 (4mM) (Sigma Chemical Co., St Louis, MO) was also included to suppress fast sodium currents. Osmolarity was adjusted to 270-290 mOsm. Pipette resistances generally were in the

range of 4-7M Ω. 0.3~ 0.4% Biocytin (Sigma Chemical Co., St Louis, MO) was also added to the intracellular solution for later visualization of the morphology of the recorded cells.

After > 1 hour of incubation in the holding chamber, the slice was transferred into a small submersion chamber maintained at room temperature (20-24°C) and secured in place with a bent piece of platinum wire resting on the top of the slice. Individual cells were visualized using an infrared differential interference contrast (IR-DIC) Zeiss Axioskop microscope and a 40X water immersion objective. Tight seals (>1G Ω) were obtained on a pyramidal-shaped cell and whole cell recordings were made after rupturing cell membrane with gentle suction. After the establishment of the whole-cell recording configuration, stable long lasting tight-seal recordings were achieved in most cases. Spontaneous and evoked IPSCs were recorded continuously using an Axopatch 1-D amplifier (Axon Instrument Inc, Foster City, CA). Output current signals were DC-coupled to a digital oscilloscope (Nicolet Model 410). Series resistance was monitored throughout the recordings and a cell was discarded if it changed significantly. In addition, a PCM/VCR recorder (Model 400, A.R. Vetter Co, Rebersburg, PA) was used to capture all tracings of synaptic events for off-line analysis and archiving. The stored signal was further analyzed using Strathclyde Electrophysiology Software Whole Cell Program (Courtesy of Dr. John Dempster) with an interface (BNC-2090, National Instruments, Austin, TX) to a PC-based computer.

Electrical stimulation

A monopolar tungsten electrode (A-M system, Inc, Carlsborg, WA) was placed about 50~70 μm lateral to the soma of the recorded pyramidal cells. The stimulus threshold was first determined by increasing intensity (5-120 μA) of rectangular wave pulse until detectable responses occurred. Then constant current rectangular stimulus pulses 4 times higher than threshold intensity with a duration of 0.1ms and interval of 0.0166Hz were delivered through the electrode by an isolated stimulator (Grass S88, Grass Instrument CO, Quincy, MA).

Histological identification of pyramidal cells.

During recording, pyramidal cells were filled with Biocytin. After the end of the recording the slice was allowed to stay in the recording chamber for an additional 10-20 minutes for biocytin transport within the axon. The slices were then placed overnight in 4% paraformaldehyde and 0.05% gultaraldehyde in 0.1M phosphate buffer saline (PBS). The slices were washed thoroughly in PBS and were incubated in 0.1 M Tris-buffered saline (TBS) containing 1% H_2O_2 for 30 minutes. The slice were then incubated with avidin-biotin-peroxidase complex (ABC kit, Vector Labs, Burlingame, CA) in TBS containing 0.05% Triton X-100 overnight at 4°C. The slices were then rinsed 3 times in PBS and then reacted in a solution containing DAB (DAB kit, Vector Labs, Burlingame, CA). The slices were then cleared and mounted. The morphology of the biocytin-filled pyramidal cells was examined under light microscope and pyramidal cells were drawn using a camera lucida.

Statistical analysis of data and drug application

Data were analyzed off-line using the Strathclyde Electrophysiological Software. The Kolmogorov-Sminove (K-S) statistical test was used to compare two different cumulative distributions using Origin 5.0 for Windows (MicroCal Software, Norththampton, MA). Paired and unpaired *t*-tests and one-way ANOVA tests were also used, when appropriate. All group data are presented as mean ± SEM.

MK-801 (dizocilpine maleate) and tetrodotoxin (TTX) were purchased from RBI (Research Biomedical International (RBI), Natick, MA). D-(-)2-amino-5-phosphonovaleric acid (D-AP5) and bicuculline methiodine (BMI) were purchased from Sigma (Sigma, St, Louis, MO). All drugs were dissolved directly into the ACSF and bath-applied in the perfusion medium.

Results

Since the pyramidal cells are found mostly between layers II and VI of the neocortex, we therefore intentionally investigated these cortical strata in the RSC. Data were acquired from 53 pyramidal cells in the RSC and 7 from the parietal cortex. Stable whole cell recordings from pyramidal cells lasted from 50 min to 3 hours. Due to the irreversible blockade of NMDA receptors by MK-801, only a single experiment was done from each cortical slice treated with MK-801.

Morphology of dendritic and axonal arbors of pyramidal cells in the RSC

The morphology of each recorded cell was examined with biocytin staining to unambiguously distinguish pyramidal cells from other cell types. In the present study, we were able to recover histologically ~90% of all recorded cells in the RSC areas. Almost all cells initially thought to be pyramidal cells on the basis of their triangular shapes of somata and long apical dendrites projecting toward the pial surface in living slice were found to be pyramidal cells, as later determined by biocytin staining. However, two cells were confirmed to be non-pyramidal cells based on their axonal and dendritic arborization; therefore, their electrophysiological and pharmacological data were not included in this study.

The somata of biocytin-filled pyramidal cells had spherical, ovoid or irregular forms. The dendritic arbor of pyramidal cells in the RSC was characterized by a long apical dendrite usually extending toward to the pial surface where it typically branched extensively to form multiple small terminal tufts just under the pial surface. Along the length of the apical dendrites are numerous oblique branch dendritic collaterals. Basal dendrites extended outward from the lower portion of the soma and ascend or descended with gradual tapering. The axonal arbor of pyramidal cells was densely distributed around the soma and also extend widely, horizontally and vertically. These morphological characteristics are consistent with cortical pyramidal cells described elsewhere (Kim and Connors 1993, Lubke et al, 1996, Feldmeyer and Sakmann 2000, Reyes and Sakmann 1999). Figure-1 shows a camera lucid reconstruction of pyramidal cells. The soma of this pyramidal cell is located in layer IV/V and it sends a long axon projecting to contralateral side across the corpus callosum (Sripanidakulchai and Wyss 1987).

MK-801 decreases spontaneous IPSC frequency of pyramidal cells in the RSC

Spontaneous IPSCs were recorded from pyramidal cells in the RSC using whole-cell voltage clamp techniques, with a holding potential of +10 or +30mV and a calculated E_{Cl} of -41mV for the internal solution used. Under these experimental conditions, the sIPSCs were inward currents at a holding potential of –70mV (Figure-2A) and were robust outward currents at a holding potential of +30mV (Figure-2B). A plot of the evoked post-synaptic currents amplitude against holding potential (Figure-2D) indicated an x-intercept of –40mV, closely approximating the calculated reversal potential of E_{CL} (Figure-2E). In addition, the recorded sIPSCs were abolished by bath application of a selective $GABA_A$

receptor antagonist, bicuculline methiodide (BMI) (20μM) (Figure-2C). These results indicated that, under these conditions, the recorded IPSCs were mediated by the activation of $GABA_A$.

Effects of MK-801 on sIPSCs of pyramidal cells recorded from the RSC are demonstrated in Figure-3 and 4. Figure-3 shows a pyramidal cell recorded from layer V and its morphology is shown in Figure-3C. At a holding potential of +30mV, the recorded IPSCs were outward currents (Figure-3A, top panel). The IPSCs were abolished by bath application of BMI (20μM) and recovered partially on washout (Figure-3A, lower panels). Bath application of the NMDA antagonist, MK-801 (40μM), caused significant decreases in the frequency and amplitudes of sIPSCs in this pyramidal cell (Figure-3A). The cumulative probability distributions for these changes were shown in Figure-3B. As shown in Figure-3B, bath application of MK-801 produced a rightward shift in the distribution of sIPSCs intervals (figure-3B, left panel), indicating a decrease in frequency (K-S test, $P<0.01$). In addition, sIPSCs amplitudes were also reduced significantly (K-S test, $P<0.001$), as shown in Figure 3B (right panel).

Figure-4 shows a pyramidal cell recorded from layer III in the RSC. Similar to the pyramidal cell shown in Figure-3, this layer III pyramidal cell also responded to bath application of MK-801 (40 μM) with a significant decrease in the frequency of sIPSCs (Figure-4A, 4B). Amplitudes of sIPSCS were also attenuated by MK-801. Although sIPSCs with a larger amplitude dominated in this layer III pyramidal cell, the morphology

of this pyramidal cell, as shown in Figure-4D, is similar to that of the pyramidal cell illustrated in Figure-3C.

We pooled data obtained from pyramidal cells recorded in layers II to VI of the RSC. When a dose of 40 μM MK-801 was employed, the mean inter-event interval was 1.06 ± 0.24s in control and 2.47 ± 0.35s after bath application of MK-801 ($p<0.05$, paired *t* test; n=12). Overall, a decrease in the frequency of sIPSCs was observed in 80% pyramidal cells after application of MK-801 (10-40 μM). In the remaining pyramidal cells, the responses to application of MK-801 varied from a slightly decrease in the frequency of sIPSCs (n=2) to no responses (n=1) to bath application of MK-801.

We also examined the concentration-dependence of MK-801-induced decreases in the frequency of sIPSCs of pyramidal cells. We used three concentration of MK-801:10, 20 and 40μM. One example of the dose dependence of the effect is shown in Figure-5. In this pyramidal cell whose soma is located in layer VI (Figure-5B), an increase in the concentration of MK-801 from 10 to 40μM results in a graded decrease in the frequency of sIPSCs as demonstrated in Figure-5A, in which cumulative inter-event intervals shift to the right. The mean inter-event intervals were 1.1 ± 0.24s in control, 1.31 ± 0.13s, 1.97 ± 0.35 and 2.43 ± 0.26 after bath application of MK-801 at the concentration of 10, 20 and 40μM, respectively ($p < 0.05$, one-way ANOVA; n=4). In addition, inhibitory effects of MK-801 on sIPSCs recorded from those cells, which were treated with only single concentration of either 10 or 40μM, were compared. As expected, 40μM of MK-801 showed greater inhibition on sIPSCs than 10μM.

In addition, we also tested the effect of a widely used competitive NMDA receptor antagonist, D-AP5. Similar to MK-801, D-AP5 (50μM) significantly decreased the frequency of sIPSCs in two pyramidal cells tested (data not shown).

MK-801 reduced amplitude of evoked IPSCs in pyramidal cells in the RSC

In these experiments, pyramidal cells were held at +5 to +30mV and an outward current was evoked a pulse delivered to the brain slice via a stimulating electrode (see Methods). These outward currents were abolished by bath application of $GABA_A$ receptor antagonist, BMI (20μM) indicating that they are mediated by $GABA_A$ receptor (Figure-6A). These currents will be referred to simply as evoked IPSCs (eIPSCs).

With the glutamatergic system uninterrupted, the evoked IPSCs were considered to be polysynaptic in origin. These polysynaptic eIPSCs could represent a direct or indirect activation of local circuitry in which GABAergic interneurons play a critical role in regulating activity of excitatory neurons (Kawaguchi 1995, Kawaguchi and Kubota 1996). The effects of MK-801 on eIPSCs were shown in Figure-6B; these responses were gradually but significantly reduced by bath applied MK-801. This effect is shown by the recording from a layer IV RSC pyramidal cell illustrated in Figure-6B. At a holding potential of +5mV, it was first recorded for 10 minutes as control before bath application of MK-801. Five minutes after addition of MK-801 (40μM), the eIPSCs began to decline,

and reached a minimum amplitude 30 minutes post-treatment. Amplitudes of eIPSCs were reduced from 1.0nA to 0.5nA (50% of control). The eIPSC was blocked by bath application of BMI (20μM) and recovered upon washing out BMI. Overall, MK–801(40μM) significantly reduced evoked responses to 51 ± 8% of control (n=14; $p<0.05$, paired *t* test). In addition, MK-801 decreased the amplitude of eIPSCs in a dose-dependent manner. The results of these experiments suggested that NMDA receptor antagonist, MK-801, reduces the evoked release of GABA from interneurons due to either a direct reduction in synaptic excitability or by a decrease in excitatory drive to interneurons in the cortex.

Comparison of effects of MK-801 on sIPSCs and eIPSCs of pyramidal cells recorded in the RSC and the parietal cortex

Several whole animal studies have demonstrated that pathomorphological changes induced by MK-801 occur in the different areas of the brain, but with different sensitivity to MK-801 among the affected areas (Olney 1990, Horvath et al, 1997). When the same dosages were administered intraperitoneally, MK-801 causes more severe damage to neurons in the RSC, compared to neuronal injury occurred in other cortical areas. To determine whether sIPSCs and eIPSCs in pyramidal cells recorded from the RSC were more greatly inhibited than those recorded from other brain regions, we recorded sIPSCS from 7 pyramidal cells in the parietal cortex, an area less sensitive to MK-801-induced damage in vivo studies (Olney et al, 1991, Hovrath et al 1997). We chose to use 40μM

MK-801 in order to evoke a maximum inhibitory effect on sIPSCs of pyramidal cells in the RSC and parietal cortex.

Similar to inhibitory effects observed in the RSC, MK-801 also reduced the frequency of sIPSCs of pyramidal cells in the parietal cortex. Figure-7 shows the effect of MK-801 on sIPSCs of a parietal pyramidal cell, whose soma was located in layer V (Figure-7C). sIPSCs were bicuculline-sensitive and were reduced by MK-801 (40μM) (Figure-7A). MK-801 significantly increased inter-event intervals (K-S test, $P<0.05$, Figure-7B, left panel), but had no significant effect on cumulative amplitude distribution (K-S test, $P>0.05$ Figure-7B. right panel). Overall, MK-801 significantly reduced sIPSCs in only 4 out of 7 (57%) pyramidal cells in the parietal cortex, compared to 80 % of those in the RSC areas. Furthermore, among the remaining pyramidal cells, MK-801 slightly, but not significantly decreased sIPSCs in 2 and had no effect on another cell. Figure-8A shows that there is a significantly great depression of sIPSC frequency by MK-801 in the RSC vs. the parietal cortex (Unpaired t-test, $P<0.05$), indicating that MK-801 caused a greater disinhibition of pyramidal cells in the RSC.

Similar results were also found on evoked IPSCs of pyramidal cells in the parietal cortex (Figure-8B). At a holding potential of +30mV, the average amplitude of eIPSCs was decreased to 72 ± 5.9%(n=5) of control after bath application of 40 μM of MK-801. However, under the same conditions, the mean amplitude of eIPSCs of pyramidal cells recorded from the RSC was decreased to 52% ± 6.4% (n=8) of control. There is significant difference between two groups ($P<0.05$, unpaired *t* test).

MK-801 did not inhibit mIPSCs of pyramidal cells in the RSC

The results described above demonstrated that a block of the NMDA receptor by antagonist MK-801 reduced $GABA_A$-receptor mediated IPSCs in RSC pyramidal cells. In order to distinguish if the decrease of sIPSCs and eIPSCs in pyramidal cell was due to a reduction of action potential dependent or action potential independent mechanisms, we used tetrodotoxin (TTX), a Na+ channel blocker, to block those synaptic events that are dependent on action potentials. Under such conditions, synaptic responses obtained in the presence of TTX will be referred to as miniature IPSCS (mIPSCs).

We have investigated the effect of MK-801 on mIPSCs of 5 pyramidal cells in the RSC and found that MK-801 did not affect mIPSC frequency or amplitude. Figure-9A demonstrates sIPSCs recorded from a pyramidal cell in layer III before and after application of TTX (0.5μM). As this figure shows, TTX caused a decrease in the average sIPSCs amplitude, indicating that significant portion of the sIPSCs was due to action potential-dependent GABA release from inhibitory interneurons. In the presence of TTX and at a holding potential of +30mV, the average frequency of mIPSCs of pyramidal cells was 4.5 ± 0.26/s and the mean amplitude was 35 ± 6.2pA (n=5). After pretreatment of a cortical slice with TTX for more than 30min, bath application of MK-801 (40 μM) had no effect on the frequency and amplitude of mIPSCs (Figure-9A). In contrast to the effects of MK-801 on spontaneous IPSCs, there was no significant change neither in cumulative probability distribution of the frequency (Figure-9B, left panel) nor amplitude

of mIPSCs (Figure-9B, right panel) after bath application of MK-801 (K-S, $P>0.05$,). These results indicated that MK-801 exerts its inhibitory effect on IPSCs of pyramidal cells through an action potential dependent mechanism.

Discussion

Using whole-cell patch clamp techniques combined with morphologically identification of neurons in a brain slice preparation, we have investigated the effect of the non-competitive NMDA receptor antagonist MK-801 on spontaneous and evoked inhibitory post-synaptic currents in the pyramidal cells in the RSC of male rats. The results of the present study demonstrate that $GABA_A$ receptors-mediated synaptic transmission in cortical pyramidal cells is modulated by MK-801 through blockade of NMDA receptor mediated events. These observations suggest that NMDA receptors mediated excitation of interneurons facilitates spontaneous and evoked GABAergic inhibition of pyramidal cells in the retrosplenial cortex.

The modulation of GABAergic inhibition by MK-801 parallels the regional neurotoxicity of MK-801 in vivo models

MK-801 has neuroprotective effects in certain CNS disorders (Foster et al,1988; Dirnagl et al, 1990, Tomitaka et al, 2000), but MK-801 also affects cognition (Sams-Dodd 1997) and temperature regulation (Colbourne et al, 1999). Furthermore, neurotoxic effects are induced by prolonged MK-801 blockage of NMDA receptors. Several independent studies have confirmed that chronic injection of a low dosage of MK-801 or phencyclidine (PCP) into the rats causes a vacuolization of neuronal cytoplasm in the posterior cingulate cortex/retrosplenial cortex, but this vacuolization may reflect transient, not permanent neurotoxicity. However, severe or irreversible neuronal damage usually occurs following a high dose or repetitive administration of a low dosage (Olney

et al, 1989, Horvath et al,1997). In these studies, there are clear regional differences in the susceptibility to MK-801 neurotoxicity. The RSC is found to be more susceptible to MK-801 than other cortical areas insults (Olney et al 1989, Horvath et al, 1997) with larger numbers of degenerating cells observed in this area in silver stains (Horvath et al, 1997).

In our study, we also found evidence of regional differences in the disinhibitory effects of MK-801 that are similar to those seen in histological studies. When 40μM of MK-801 was used, sIPSCs of pyramidal cells in RSC were significantly decreased, whereas sIPSCs recorded in pyramidal cells of the parietal cortex. Although it is unknown what causes this selective vulnerability in different brain regions, the largest increase in glucose utilization after MK-801 treatment occurs in the entorhinal and cingulate areas (Nehls et al, 1990, Kurumaji and McCulloch, 1990, Patel and McCulloch 1995) suggesting that these areas may be more disinhibited by the drug than other cortex. Although our electrophysiological data cannot confirm the selective vulnerability to cell injury in different brain regions, they provide a potential mechanism to help explain the selective injury to the RSC if indeed MK-801 produces greater disinhibition in the RSC than in other cortical areas.

MK-801 modulates IPSC of pyramidal cells via a presynaptic mechanism

Reduction of inhibitory transmission by NMDA receptor blockade has been observed in CA1 neurons in the hippocampus (Hablitz and Langmoen, 1986, Cruntz et al, 1996) and

the basolateral amygdala (Rainnie et al, 1991). In rat olfactory bulb, activation of NMDA receptors is required to dendrodendritic inhibition (Schoppa et al, 1998). These investigators suggested that the reduction in inhibitory transmission resulted from a loss of excitatory drive to interneurons in the local circuit.

Our findings are also compatible with this mechanism. MK-801 definitely reduced the frequency of sIPSCS and the amplitude of eIPSCs, but did not affect the frequency or amplitude of TTX insensitive mIPSCs. This argues that MK-801 did not affect the postsynaptic efficiency of released GABA and did not affect quantal size or probability of spontaneous release (Cohen et al 1992, Hoffman and Lupica 2000). MK-801 seemed to affect only action potential dependent GABA release compatible with an effect on either action potential induced calcium influx to the presynaptic terminal or an effect on action potential initiation or propagation in inhibitory interneurons. Consequently, our future experiments will focus on recording the effects of MK-801 on the synaptic currents and resting spontaneous activity of interneurons.

Functional implications for disinhibition of cortical interneurons and its role in neuronal death

Although there is a functional diversity in these cortical pyramidal cells, these glutamatergic excitatory pyramidal cells and GABAergic interneurons form cortical networks, in which pyramidal cells send excitatory drive to GABAergic interneurons via excitatory axon collaterals. GABAergic interneurons also have axon collaterals projected

back to the apical dendrites of pyramidal cells to form reciprocal connections (Markram et al, 1998, Reyes et al, 1998) Through this network, intrinsic excitability of apical dendrites of pyramidal cells are regulated by inhibitory inputs since the spiking patterns of apical dendrites are modified by IPSPs recorded from the apical dendrites (Kim et al, 1995). In our study, pyramidal cells recorded and filled with biocytin show long apical dendrites projecting to surface of the pia with many oblique dendrite branches. By preventing excitatory drive to inhibitory circuits in the neocortex, one would expect an attenuation of tonic inhibitory control over other cortical cells, including acetylcholine-containing cells. For example, blockade of glutamatergic hippocampal-setptal pathway by MK-801 results in a decrease in GABA outflow and an increase of acetylcholine outflow in rat (Giovannini et al 1994). Therefore, the above mechanism could play an important role in mediating neurotoxic effects induced by the enhanced cholinergic activity caused by organophosphorous nerve agents such as sarin and soman. Therefore, any attempts to prevent neuronal injury by administration of NMDA receptor antagonists could worse neurodegenation or promote brain cells death to the subjects who have already exposed to a chemical compound. This may well be the case during the wartime on military personnel or a biological attack on civilians during the peace-time.

In summary, previous neurotoxilogical studies (Olney et al, 1989, 1991,) have confirmed MK-801-induced neuronal injury. Based on electrophysiological analysis of inhibitory postsynaptic currents recorded from morphologically identified pyramidal cells in rat RSC, we have demonstrated that NMDA receptor antagonist MK-801 reduced IPSCs of pyramidal cells. The effects of MK-801 on pyramidal cells IPSCs are thought to be

through a direct action on pre-synaptic terminals of Gabaergic interneurons by affecting GABA releases. Our electrophysiological finding supports the notion that blockage of NMDA receptors by MK-801 or other NMDA receptor antagonists attenuate or diminish glutamatergic neurons-activated tonic inhibition and disrupts the inhibitory control over other neurons. One of most important implications regarding MK-801 induced neurotoxicity to brain cells is that loss of $GABA_A$-mediated inhibition (or disinhibition) could facilitate massive release of acetylcholine from cholinergic neurons in the brain and leads to neuronal death.

Future study

Effect of MK-801 on excitatory postsynaptic currents (EPSCs) in cortical interneurons

Significance of work:

Our electrophysiological data for the first time indicated that excitatory drive from excitatory pyramidal cells to inhibitory interneurons can be modulated by MK-801. MK-801 seemed to affect only action potential dependent GABA release compatible with an effect on either action potential induced calcium influx to the presynaptic terminal or an effect on action potential initiation or propagation in inhibitory interneurons.

Consequently, our future experiments will focus on recording the effects of MK-801 on the synaptic currents and resting spontaneous activity of interneurons.

Figure Legends

Figure 1 Camera lucida reconstruction of an RSC pyramidal cell filled with biocytin

Camera lucida reconstruction of a pyramidal cell recorded in the RSC. This pyramidal cell was filled with biocytin during the experiment. The soma of the pyramidal cell is located in layer V. An apical dendrite arising from the soma extends toward to the pia surface and branches off to form multiple tufts. In addition to a typical apical dendrite arborization, a long axon originating from the soma extends about 2896 micrometers and projects to contralateral side of the hemisphere through the callosum. One of branches of the axon projects ispilaterally to the lateral cortex. The pia is near the end of apical dendrite branches. cc: Corpus Callosum. Dashed lines: approximate pial surface of the cortex. Calibration bar: 200μm.

Figure 2 $GABA_A$ receptor mediated IPSCs of pyramidal cells

Whole cell recordings were performed using a CsCl-based internal solution at holding potentials of -70mV (A) and +30mV(B). When the holding potential was –70mV, inward currents were recorded while the currents become outward as cell was held at +30mV. The $GABA_A$ receptor antagonist, bicuculline methiodine (BMI) (20μM) abolishes the current (C). Amplitudes of evoked IPSCs recorded from another pyramidal cell, which was held at different potentials of –70 to + 20mV. (D) Base on the evoked synaptic responses shown in Figure-D, an I-V curve (E) was constructed and revealed an apparent reversal potential of -40mV, which was near the calculated E_{CL} equilibrium potential. These findings indicate that recorded IPSCs were mediated by $GABA_A$ receptors. Calibration bar: 500ms/0.1nA.

Figure 3 Effect of MK-801 on spontaneous $GABA_A$ receptor mediated IPSCs in RSC pyramidal cells

A. MK-801 decreases sIPSCs frequency and amplitude in an RSC pyramidal cell. At holding potential of +30mV, bath application of MK-801 (40μM) decreases sIPSCs. Recorded sIPSCs were abolished by BMI (20μM) and recovered after washout. Calibration: 500ms/0.1nA

B. Cumulative inter-event interval distribution for the same cell shows a significant increase in the inter-event interval ($P<0.01$, K-S test). Cumulative amplitude distribution also shows a significant decrease in the amplitude ($p<0.001$, K-S test).

C. Photomicrograph of the same cell filled with biocytin was shown. Calibration bar 100 μm.

Figure 4 Effect of MK-801 on sIPSCs in another RSC pyramidal cell

At the holding potential of +30mV, bath application of MK-801 (40μM) (B) decreases sIPSCs compared to control (A). Recorded sIPSCs were abolished by BMI (20μM) (C). Calibration: 500ms/0.1nA.

D. Camera lucida reconstruction of the same pyramidal cell recorded in the RSC was shown. Calibration bar 100μm.

Figure 5 Effect of MK-801 on sIPSCs of pyramidal cell in the RSC is concentration-dependent

A. At holding potential of +30mV, bath application of MK-801 (10, 20 and 40μM) caused a graded decrease in the frequency in sIPSCs. Cumulative inter-event interval distribution for the same cell shows a significant increase in the inter-event interval ($P<0.01$, K-S test).

B. Photomicrograph of the same pyramidal cell filled with biocytin was shown. Calibration bar 100μm.

Figure 6 Effect of MK-801 on eIPSCs of pyramidal cells in the RSC

A. Outward IPSCs were recorded from a pyramidal cell at a holding potential of +30mV and were completed blocked by BMI (20 μM). In addition, the evoked IPSC were fully recovered after washout, indicating that recorded IPSCs were mediated by $GABA_A$ receptor. Calibration bars: 50mS/0.1nA.

B. The time course of evoked IPSC of another pyramidal cell, after bath application of MK-801 (40 μM), BMI (20μM) and washout, respectively. Insets show the averaged peak IPSC traces corresponding to each treatment.

C. Photomicrograph of the same cell filled with biocytin was shown. Calibration bar 100μm.

Figure 7 Effect of MK-801 on sIPSCs of a pyramidal cell in the parietal cortex

A. At the holding potential of +30mV, bath application of MK-801 (40μM) decreased sIPSCs. Recorded sIPSCs were abolished by BMI (20μM) and recovered after washout. Calibration: 500ms/0.1nA.

B. Cumulative inter-event interval distribution for the same cell shows a significant increase in the inter-event interval ($P<0.05$, K-S test). As shown by cumulative amplitude distribution, MK-801 did not significantly decrease in the IPSC amplitude ($p>0.05$, K-S test).

C. Photomicrograph of the same cell filled with biocytin was shown. Calibration bar 100μm.

Figure 8 Comparison of MK-801 on sIPSCs of pyramidal cells in the RSC and the parietal cortex

A. Graph shows data from the averaged inter-event intervals of 12 pyramidal cells recorded in the RSC and 7 in the parietal cortex. MK-801 (40μM) significantly increased the average sIPSCs inter-event interval of pyramidal cell in the RSC compared to those in the parietal cortex ($P < 0.05$, unpaired t-test).

B. Graph shows that MK-801 (40μM) significantly inhibits the average peak amplitude of eIPSCs in pyramidal cells (n=8) in the RSC compared to those in the parietal cortex (n=5) ($p < 0.05$, unpaired t-test).

Figure 9 Effect of MK-801 on mIPSCs of a pyramidal cell in the RSC

A. At the holding potential of +30mV, bath application of TTX (0.5μM) abolished all action potential dependent IPSCs. However, bath application of MK-801 (40μM) has no effect on mIPSCs.

B. Cumulative inter-event and amplitude distributions did not show any significant change ($P > 0.05$, K-S test), indicating the presynaptic action of MK-801. Calibration: 500ms/0.05nA.

C. Photomicrograph of the same cell filled with biocytin was shown. Calibration bar 100μm.

Acknowledgement

This work was supported by grants from Department of Defense (DOD, DAMA17-99-1-9541) to W.A.W, S.C and D.V.L., the Department of Veteran Affairs to W.A.W and National Institute of Health (NIH, DA-06735) to D.V.L.

References

Aitken PG, Balestrino M, Somjen GG (1988) NMDA antagonists: lack of protective effect against hypoxic damage in CA1 region of hippocampal slice, Neurosci Lett. 89: 187-192.

Allen HL, Iversen LL(1990) Phencyclidine, dizocilpine and cerebrocortical neurons. Science 247:221.

Avoli M, Oliver A (1987) Bursting in human epileptogenic neocortex is depressed by an N-methyl-D-aspartate antagonist. Neurosci Lett 76: 249-258.

Cohen GA, Doze VA, Madison DV (1992) Opioid inhibition of GABA release from presynaptic terminals of rat hippocampal interneurons. Neuron. 9: 325-335.

Colbourne F, Rakic D, Auer RN (1999) The effects of temperature and scopolamine on N-methyl-D-aspartate antagonist-induced neuronal necrosis in the rat. Neuroscience. 90:87-94.

Cummings JL (1993) Frontal-subcortical circuits and human behavior. Arch Neurol 50:873-880.

Dirnagl U, Tanabe J, Pulsinelli W(1990) Pre- and post-treatment with MK-801 but not pretreatment alone reduces neocortical damage after focal cerebral ischemia in the rat. Brain Res. 527:62-68.

Feldmeyer D, Sakmann B (2000) Synaptic efficacy and reliability of excitatory connections between the principal neurons of the input (layer 4) and output layer (layer 5) of the neocortex. J. Physiol. 525:31-39.

Fix AS, Horn JW, Writhman KA, Johnson CA, Long GG, Storts RW, Farber N, Wozniak DF, Olney JW (1993) Neuronal vacuolization and necrosis induced by the noncompetitive N-methyl-D-aspartate (NMDA) antagonist MK(++801 (Dizocilpine Maleate): A light and electron microscopic evaluation of the rat retrosplenial cortex. Exp Neurol 123:204-215.

Fix AS, Wozniak DF, Truex LL, McEwen M, Miller JP, Olney JW (1995) Quantitative analysis of factors influencing neuronal necrosis induced by MK-801 in the rat posterior cingulate/retrosplenial cortex. Brain Res. 696: 194-204.

Ford LM, Sanberg PR, Norman AB, Fogelson MH(1989). MK-801 prevents hippocampal neurodegeneration in neonatal hypoxic-ischemic rats. Arch Neurology. 46:1090-1096.

Foster AC, Gill R, Woodruff GN (1988) Neuroprotective effects of MK-801 in vivo: selectivity and evidence for delayed degeneration mediated by NMDA receptor activation. J Neurosci. 8:4745-54.

Giovannini MG, Mutolo D, Bianchi L, Michelassi A, Pepeu G(1994) NMDA receptor antagonists decrease GABA outflow from the septum and increase acetylcholine outflow from the hippocampus: a microdialysis study. J. Neurosci. 14: 1358-1365.

Grunze HCR, Rainnie DG, Hassselmo ME, Barkai E, Hearn EF, McCarley RW, Greene RW (1996) NMDA-dependent modulation of CA1 local circuit inhibition. J. Neurosci 16: 2034-2043.

Hablitz JJ, langmoen IA(186) N-methyl-D-aspartate receptor antagonist reduce synaptic excitation in the hippocampus. J Neurosci. 6:102-106.

Hoffman AF, Lupica CR (2000) Mechanism of cannabinoid inhibition of $GABA_A$ synaptic transmission in the hippocampus. J. Neurosci. 20: 2470-2479.

Horvath ZC, Czopf J, Buzsaki G (1997) MK-801-induced neuronal damage in rats. Brain Res. 753: 181-195.

Kawaguchi Y (1995) Physiological subgroups of nonpyramidal cells with specific morphological characteristics in layer II//III of rat frontal cortex. J. Neurosci. 15: 2638-2655.

Kawaguchi Y, Kubota Y (1996) Physiological and morphological identification of somatostatin- or vasoactive intestinal polypeptides-containing cells among GABAergic cell subtypes in rat frontal cortex. J. Neurosci. 16: 2701-2715.

Kim HG, Connors BW (1993) Apical dendrites of the neocortex: Correlation between sodium-and calcium-dependent spiking and pyramidal cell morphology. J Neurosci. 13: 5301-5311.

Kim HG, Beierlein M, Connors BM (1995) Inhibitory control of excitable dendrites in neocortex. J. Neurophysiol. 74: 1800-1814.

Kurumaji A, McCulloch J(1990) Effects of unilateral intrahippocampal injection of MK-801 upon local cerebral glucose utilisation in conscious rats. Brain Res. 518:342-634

Li Q, Clark S, Wilson WA, Lewis DV (2000) MK-801, an NMDA receptor antagonist, modulates the inhibitory postsynaptic currents (IPSCs) in pyramidal neurons in the rat cingulate cortex. Soc Neurosci Abstr. 2000 29:431.

Lubke J, Markram H, Frotscher, M, Sakmann B(1996) Frequency and dendrite distribution of autopses established by layer 5 pyramidal neurons in the developing rat

neocortex: Comparison with synaptic innervation of adjacent neurons of the same class. J. Neurosci. 16: 3200-3218.

Markram H, Wang Y, Tsodyks M (1998) Differential signaling via the same axon of neocortical pyramidal neurons. PNAS 95: 5323-5328.

Mott DD, Li Q, Okazaki MM, Turner DA, Lewis DV (1999) GABAB-Receptor-Mediated Currents in Interneurons of the Dentate-Hilus Border. J Neurophysiol 82:1438-1450.

Nehls DG, Park CK, MacCormack AG, McCulloch J(1990) The effects of N-methyl-D-aspartate receptor blockade with MK-801 upon the relationship between cerebral blood flow and glucose utilisation. Brain Res. 511:271-279.

Olney JW, Labruyere J, Price MT (1989) Pathological changes induced in cerebrocortical neurons by phencyclidine and related drugs Science 244:1360-1362.

Olney JW, Labruyere J, Wang G, Wozniak DF, Price MT, Sesma MA (1991) NMDA antagonist neurotoxicity: mechanism and prevention. Science 254:1515-1518.

Olney JW, Farber NB(1995) Glutamate receptor dysfunction and schizophrenia. Arch Gen Psychatry. 52:998-1007.

Patel TR. McCulloch J(1995) AMPA receptor antagonism attenuates MK-801-induced hypermetabolism in the posterior cingulate cortex. Brain Res. 686:254-258.

Paxinos G, Watson C (1986) The rat brain in stereotaxic coordinates. Academic Press, New York.

Rainnie DG, Asprodini, EK, Shinnick-Gallagher P (1991) Excitatory transmission in the basolateral amygdala. J. Neurophysiol. 66: 986-998.

Reyes A, Sakmann B (1999) developmental switch in the short-term modification of unitary EPSPs evoked in layer 2/3 and layer 5 pyramidal neurons of rat neocortex. J. Neurosci. 19: 3827-3835.

Reyes A, Lujan A, Rozov A, Burnashev N, Somogyi P, Sakmann B(1998) Target-cell-specific facilitation and depression in neocortical circuits. Nature Neuroscience 1:279 – 285.

Rod MR, Auer RN (1989) Pre- and post-ischemic administration of dizocilpine (MK-801) reduces cerebral necrosis in the rat. Can J Neurological Science. 16:340-344

Rothman SM, Olney JW (1986) Glutamate and the pathophysiology of hypoxic – ischemic brain damage. Ann Neurol 19: 105-111.

Rothman SM, Olney JW (1987) Excitotoxicity and the NMDA receptor. TINS 10: 299-302.

Sams-Dodd F (1997) Effects of novel antipsychotic drugs on phencyclidine-induced stereotyped behavior and social isolation in the rat social interaction test. Behav Pharmacol. 8: 196-215.

Schoppa NE, Kinzie M, Sahara Y, Segerson TP, Westbrook GL(1998) Dendrodendritic inhibition in the olfactory bulb is driven by NMDA receptors. J Neurosci 18:6790-6802.

Sripanidkulchai K, Wyss JM (1987) The laminar organization of efferent neuronal cell bodies in the retrosplenial granular cortex. Brain Res. 406: 255-269.

Tomitaka M, Tomitaka s, Raidev S, Sharp FP (2000) Fluoxetine prevents PCP- and MK-801-induced HSP70 expression in injured limbic cortical neurons of rats. Bio Psychiatry. 47: 838-841.

FIGURE-1

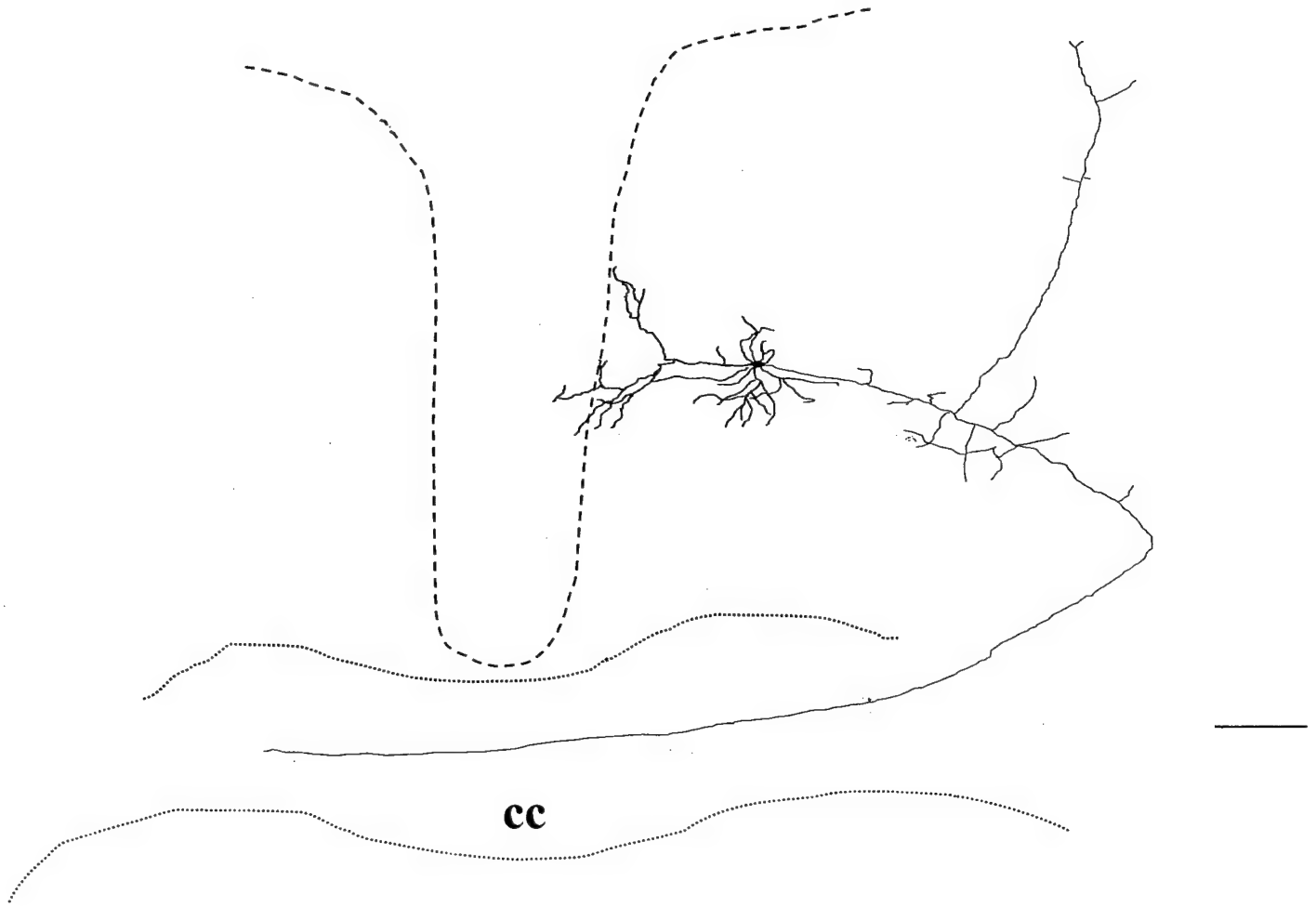

FIGURE-2

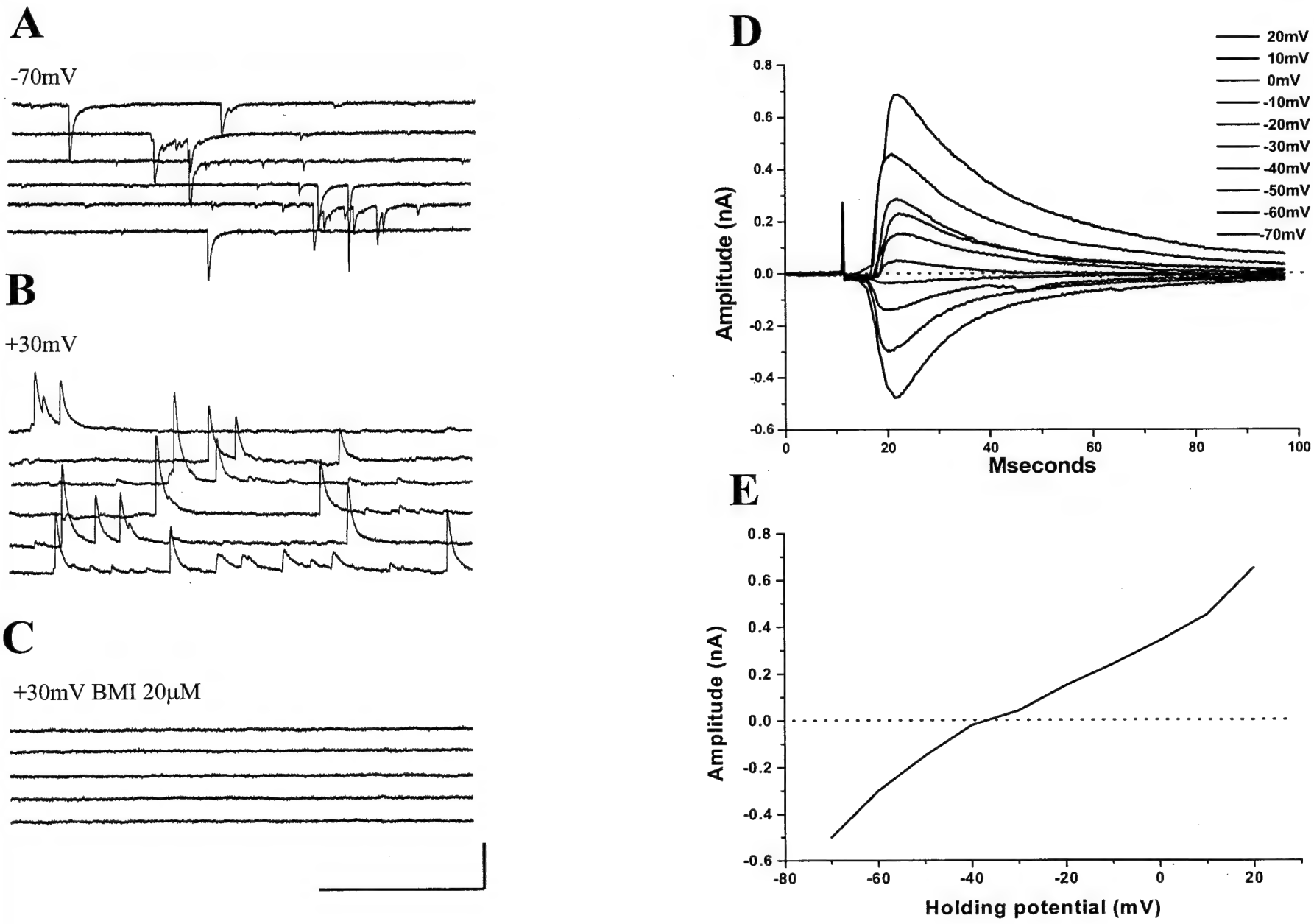
A
-70mV
B
+30mV
C
+30mV BMI 20μM
D
20mV
10mV
0mV
-10mV
-20mV
-30mV
-40mV
-50mV
-60mV
-70mV
Amplitude (nA)
Mseconds
E
Amplitude (nA)
Holding potential (mV)

FIGURE-3

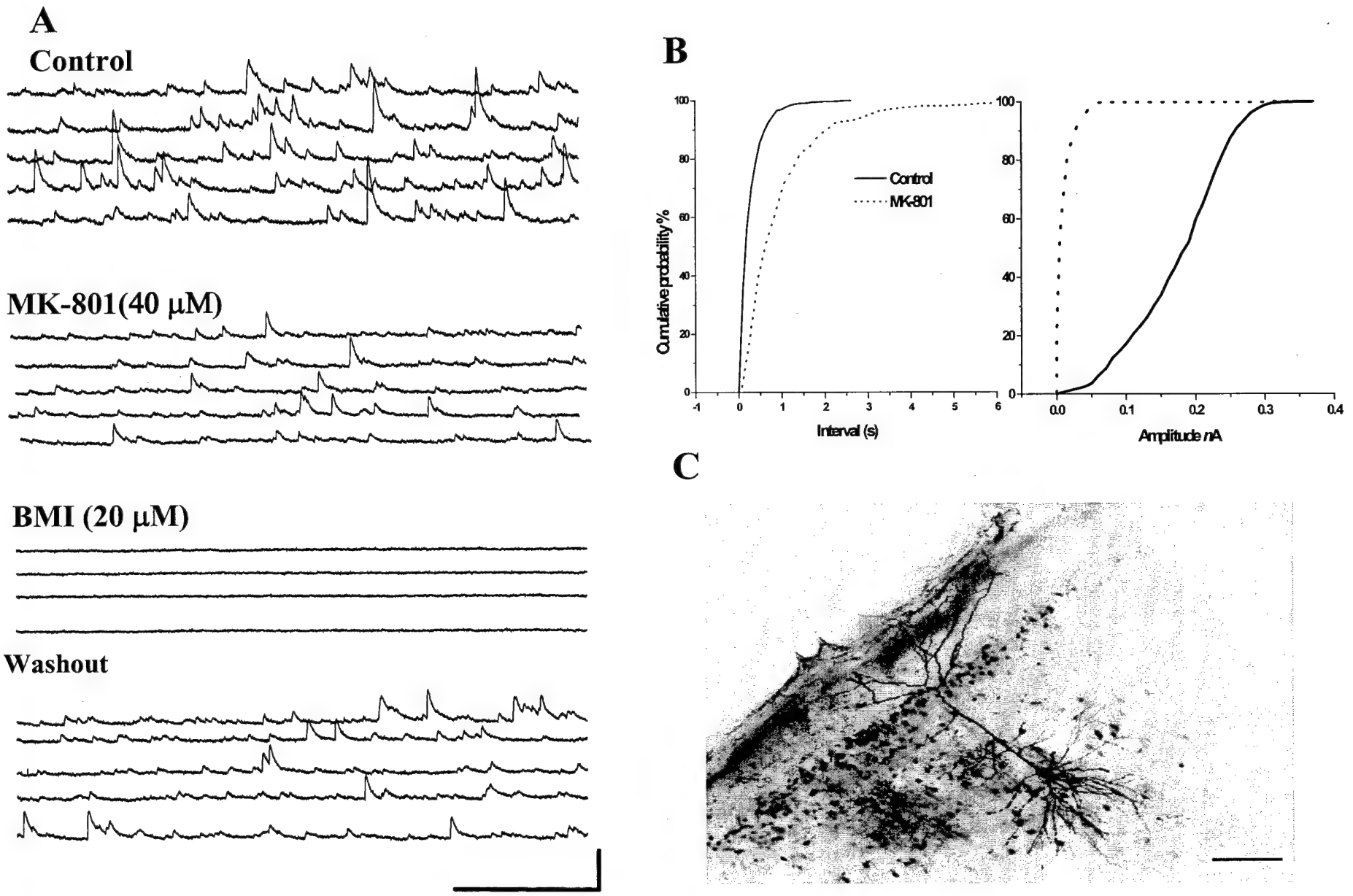
A
Control
MK-801(40 μM)
BMI (20 μM)
Washout
B
Cumulative probability %
Control
MK-801
Interval (s)
Amplitude nA
C

FIGURE-4

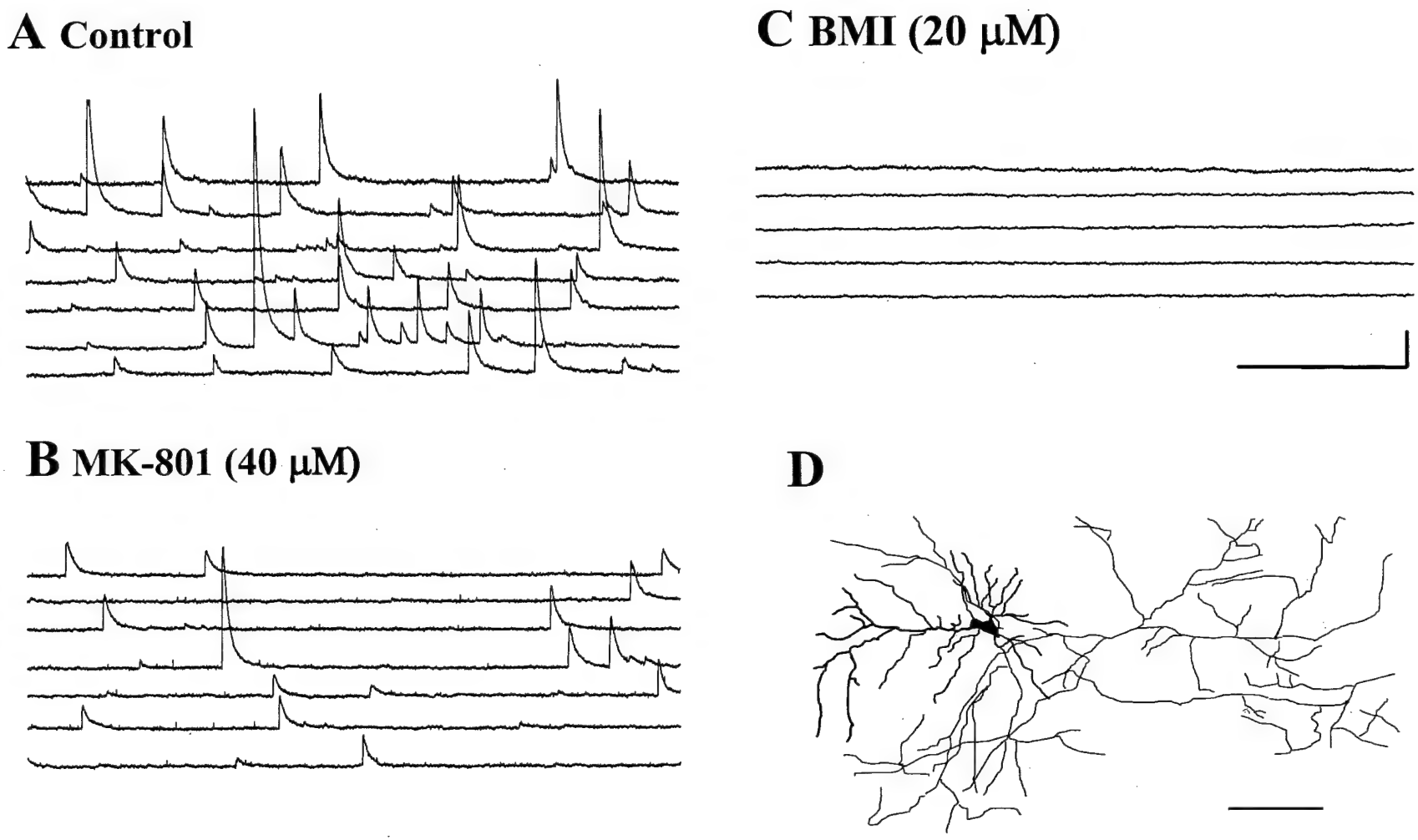

FIGURE-5

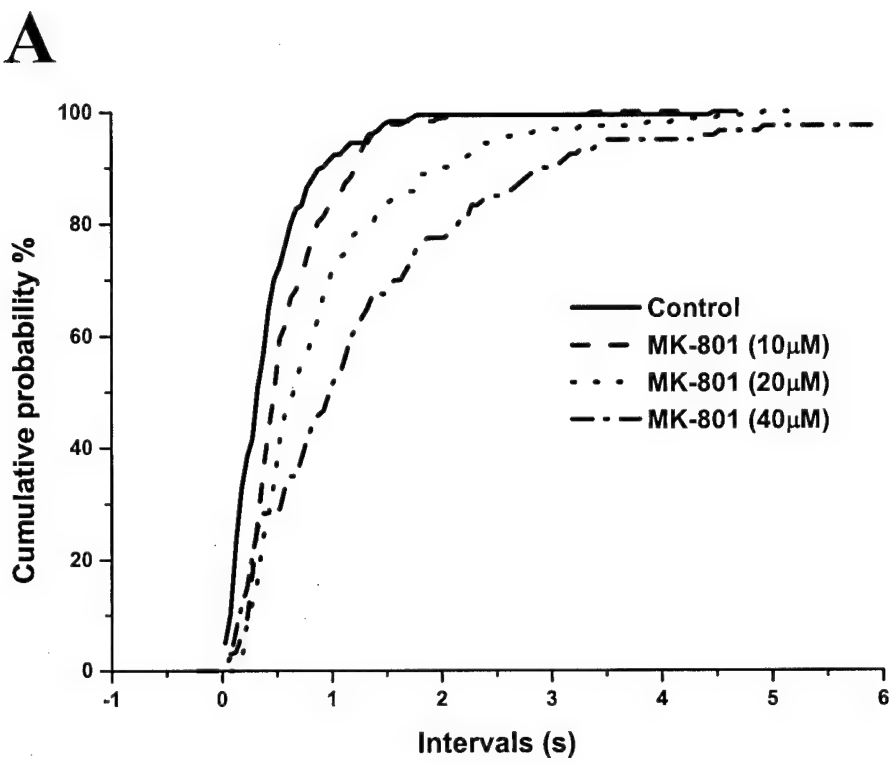
A
Cumulative probability %
100
80
60
40
20
0
-1
0
1
2
3
4
5
6
Intervals (s)
Control
MK-801 (10μM)
MK-801 (20μM)
MK-801 (40μM)

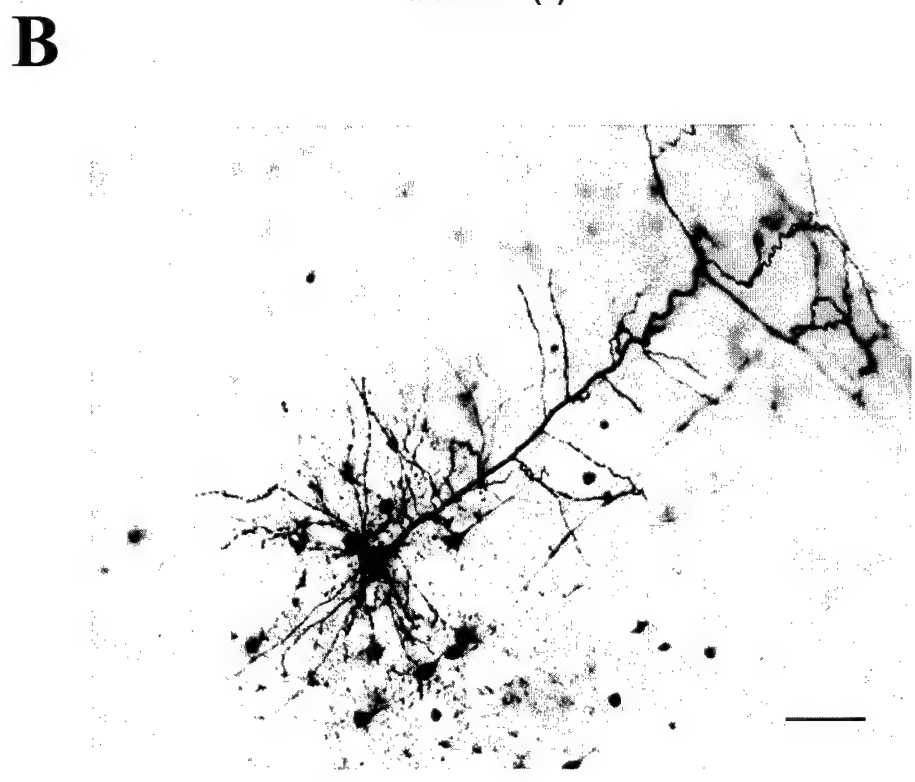
B

FIGURE-6

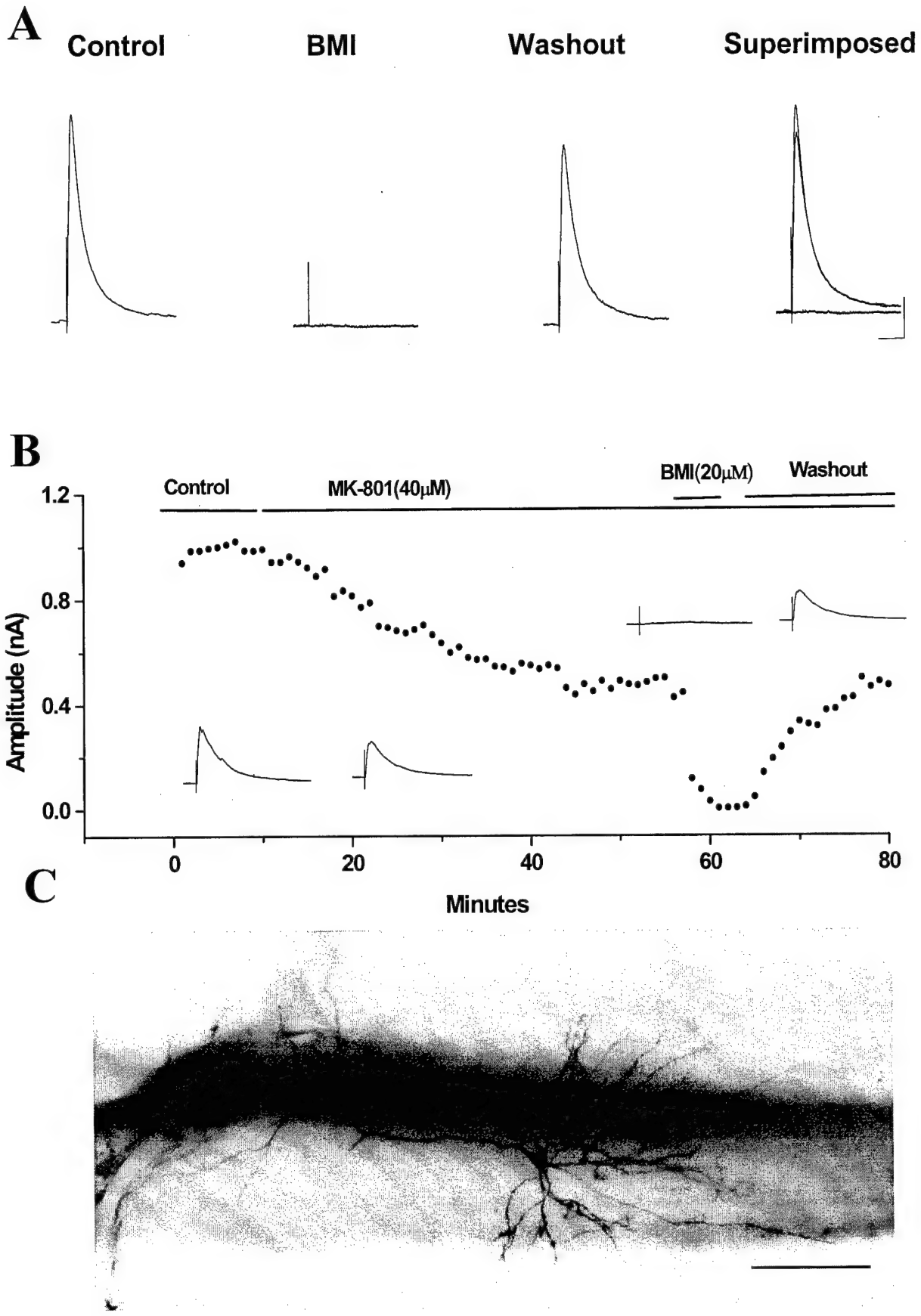
A
Control
BMI
Washout
Superimposed
B
Control
MK-801(40μM)
BMI(20μM)
Washout
Amplitude (nA)
1.2
0.8
0.4
0.0
0
20
40
60
80
Minutes
C

FIGURE-7

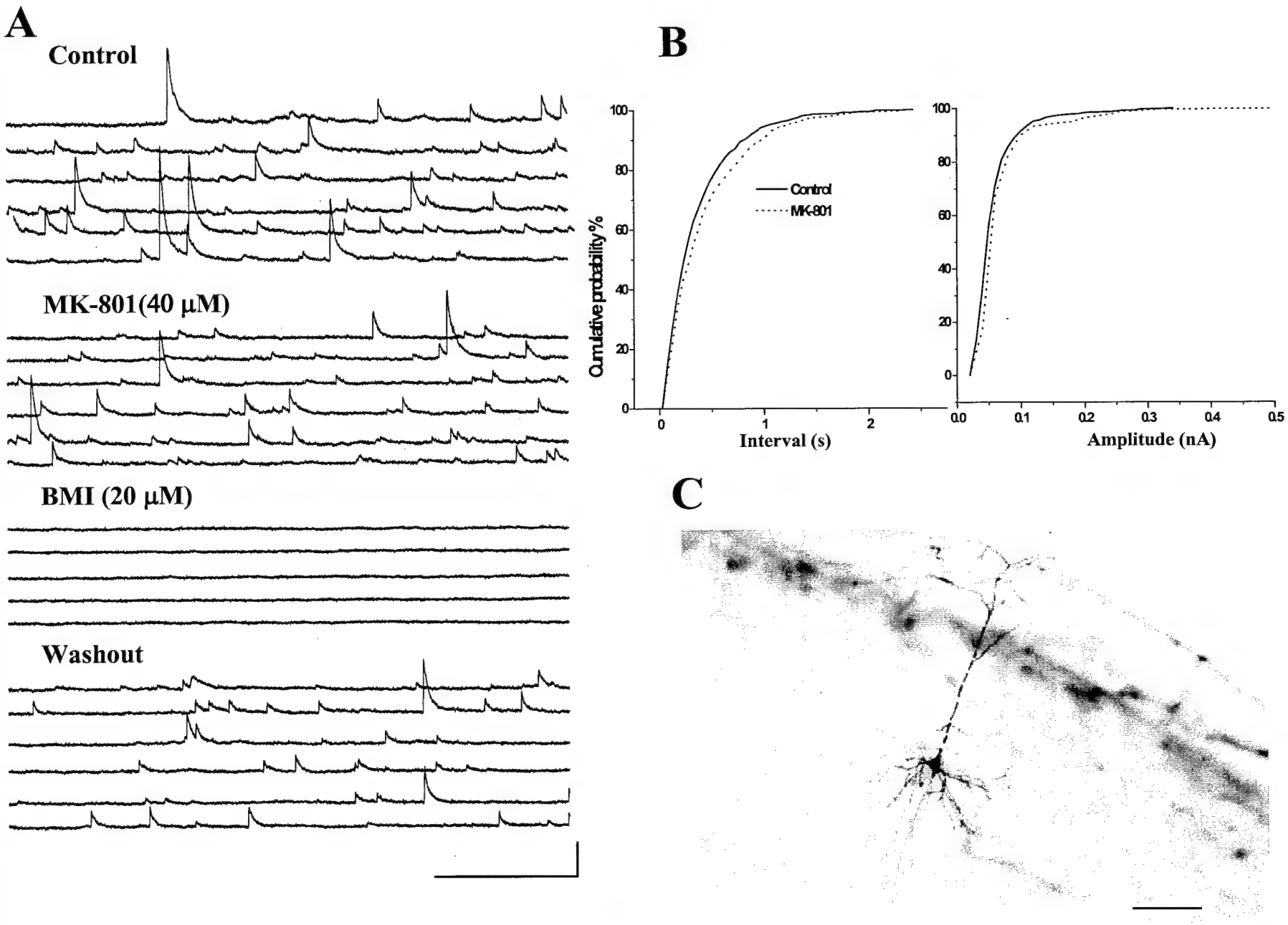
A
Control
MK-801(40 μM)
BMI (20 μM)
Washout
B
Cumulative probability %
Control
MK-801
Interval (s)
Amplitude (nA)
C

FIGURE-8

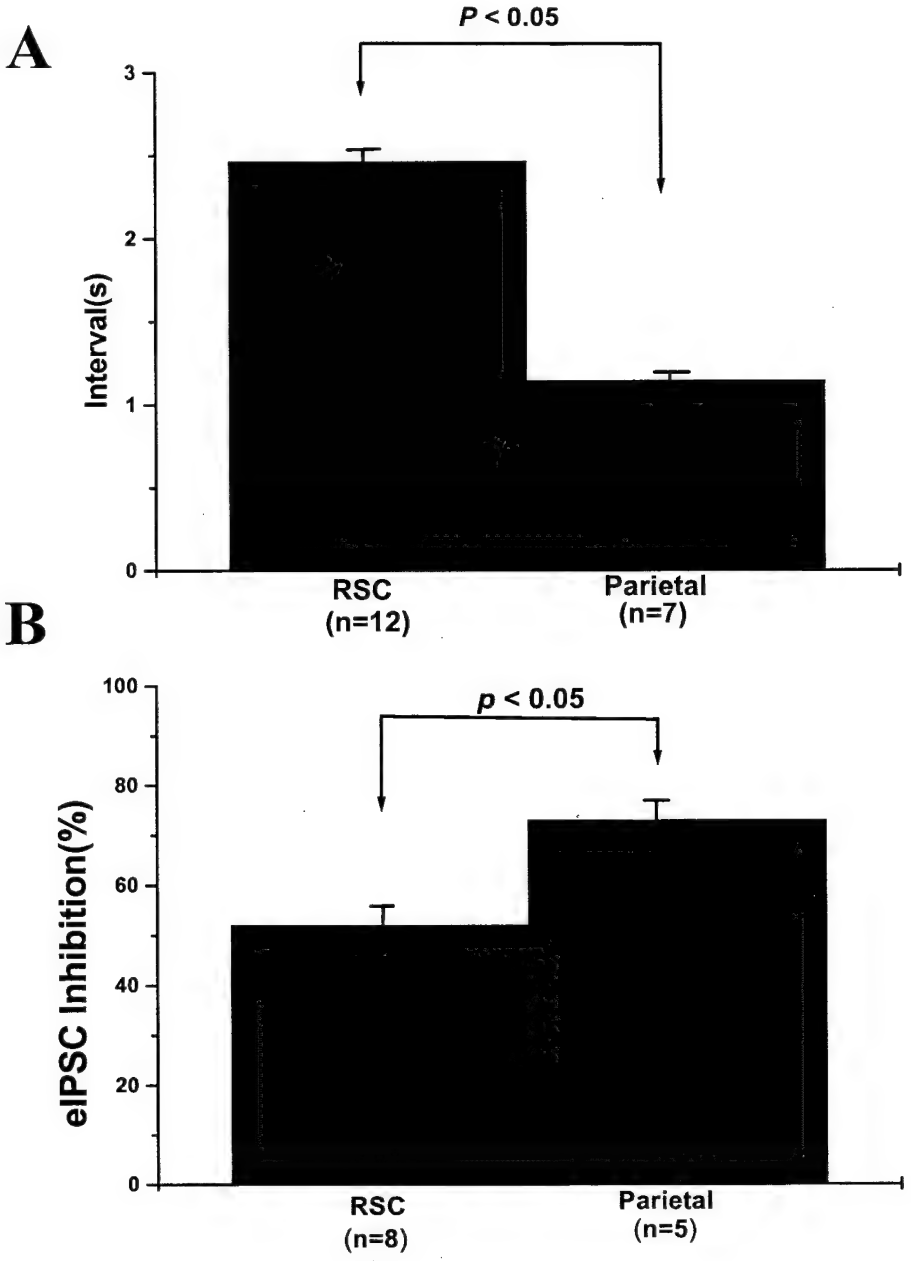
A
P < 0.05
Interval(s)
3
2
1
0
RSC
(n=12)
Parietal
(n=7)
B
p < 0.05
eIPSC Inhibition(%)
100
80
60
40
20
0
RSC
(n=8)
Parietal
(n=5)

FIGURE-9

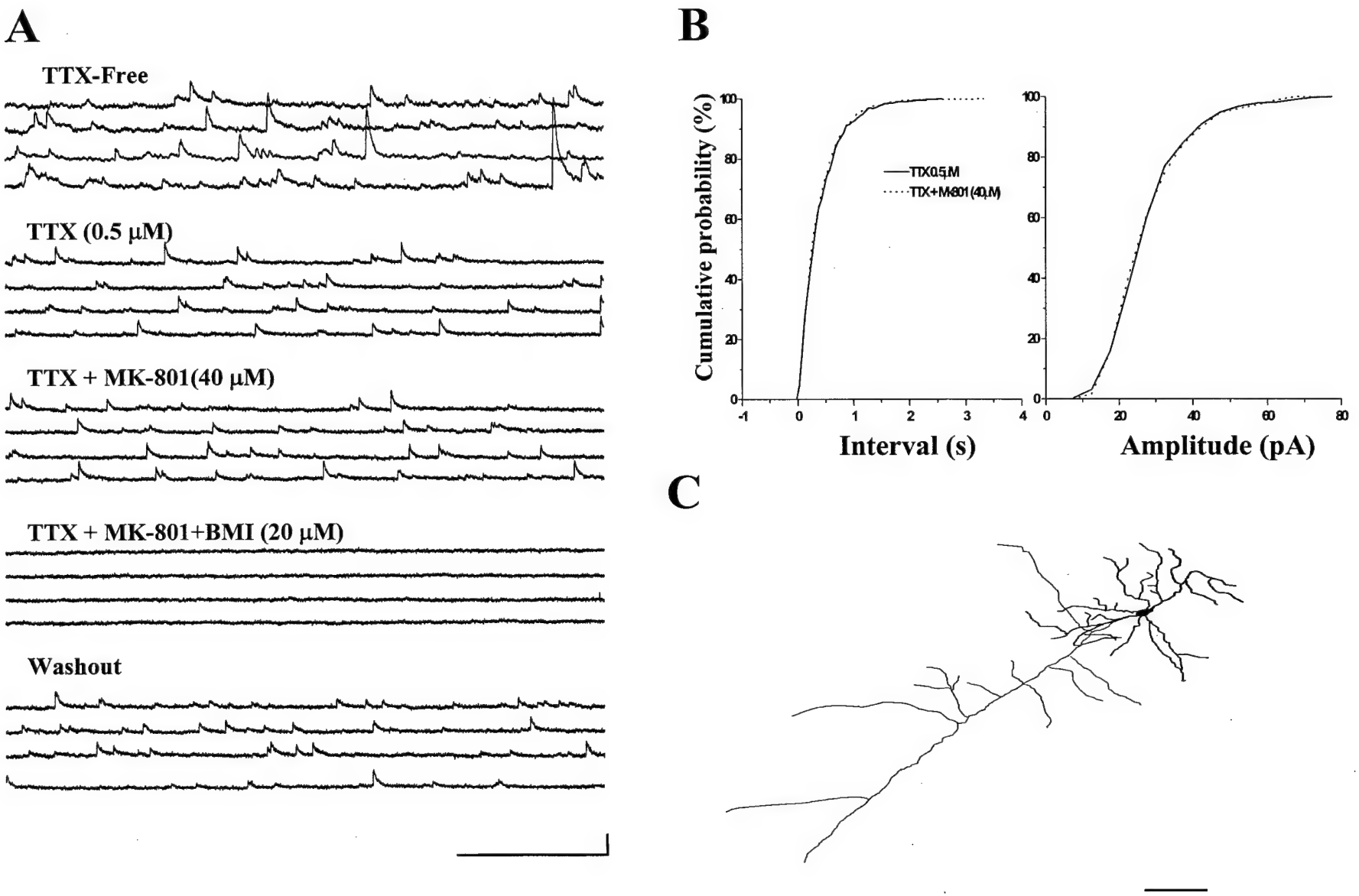
A
TTX-Free
TTX (0.5 μM)
TTX + MK-801(40 μM)
TTX + MK-801+BMI (20 μM)
Washout
B
Cumulative probability (%)
TTX0.5μM
TTX+MK801(40μM)
Interval (s)
Amplitude (pA)
C

Using Voltage Sensitive Dyes to Image the Effect of an NMDA Antagonist and Pyridostigmine in the Rat Cingulate Gyrus and Retrosplenial Cortex

Using Voltage Sensitive Dyes to Image the Effect of an NMDA Antagonist and Pyridostigmine in the Rat Cingulate Gyrus and Retrosplenial Cortex

Abstract:

We examined components of the evoked responses in the cingulate gyrus using voltage-sensitive dye imaging with a photodiode array. This relatively new technique has been successfully utilized to characterize spatiotemporal aspects of evoked and spontaneous activity in neocortex (Wu et al., 1999a; Tsau et al., 1999), olfactory bulb (Keller et al., 1998), thalamocortical pathways (Laaris et al., 2000), and amygdala formation (Wang et al., *submitted*).

Our imaging system covered a hexagonal area (1 mm facets) with each diode covering an area of 80 X 80 μm^2. This range of coverage, combined with the high temporal resolution (0.6 msec) of the photodiodes, allows recording of signal propagation along network pathways in a broad area. Accordingly, this system makes it possible to gather information from a wider anatomical area and for a longer period of time than many other recording systems, and to do so while preserving good temporal resolution.

In preliminary studies using this system, we have found that a low dose of the NMDA antagonist MK-801 (3 μM) produced an enhanced depolarization in response to a single stimulus pulse in slices from adult female rats. In contrast, pyridostigmine bromide (100 μM) was strongly inhibitory when added to a solution containing MK-801 (3 μM). This suggests that pyridostigmine may be protective against neurotoxicity caused by NMDA antagonists or, at least that pyridostigmine may not worsen the neurotoxicity of an NMDA antagonist. Thus, the combined use of these agents in clinical settings may be possible - at least within certain concentration ranges.

The importance of these results relates to the use of agents such as pyridostigmine as preventive agents against soman attacks, for individuals with soman-induced seizures may be given drugs that possess NMDA antagonist activity.

To our knowledge, this system has not been used yet to assess such neurotoxic mechanisms in the cingulate cortex, nor has it been used to assess issues of military relevance. However, it may become a powerful *in vitro* tool in which to explore neurotoxic processes to which service personnel may be at risk, and also to assess the protective potential of anti-nerve gas agents.

Key Words:

Acetylcholinesterase, MK-801, pyridostigmine, photodiode, neurotoxicity, cingulate cortex, retrosplenial cortex, Persian Gulf War

Introduction:

It is important to study the neurotoxicity of NMDA antagonists and the possible interaction of agents that affect cholinergic transmission (either acetylcholinesterase inhibitors or cholinergic agonists), for there is a very real possibility that these agents will be used together in military settings.

The *in vivo* studies discussed elsewhere in this project are providing information about cell types at risk and doses at which damage occurs. However, *in vivo* systems are fairly complicated systems in which to explore fundamental cellular mechanisms of neurotoxicity. In contrast, *in vitro* systems offer distinct advantages in such types of studies, because exact concentrations of drugs can be administered and specific anatomical regions can be monitored in detail. Also, although *in vivo* systems offer a snapshot of what happens "later" (as in, at the 3 day point after drug administration) our *in vitro* systems offer a "movie" with which to view the ongoing acute neurotoxic events that are occurring during the time of drug administration. Since much of the neurotoxicity seen at later time points is set in motion early during the exposure, such information may be helpful in understanding the mechanisms of neurotoxicity.

We examined components of the evoked responses in the cingulate gyrus using voltage-sensitive dye imaging with a photodiode array. This relatively new technique has been successfully utilized to characterize spatiotemporal aspects of evoked and spontaneous activity in neocortex (Wu et al., 1999a; Tsau et al., 1999), olfactory bulb (Keller et al., 1998), thalamocortical pathways (Laaris et al., 2000), and amygdala formation (Wang et al., *submitted*).

Our imaging system covered a hexagonal area (1 mm facets) with each diode covering an area of 80 X 80 μm^2 (Fig. 1B). This range of coverage, combined with the high temporal resolution (0.6 msec) of the photodiodes, allows recording of signal propagation along network pathways in a broad area. Accordingly, this system makes it possible to gather information from a wider anatomical area and for a longer period of time than many other recording systems - and to do so while preserving good temporal resolution.

In these first studies using this technique, we focused primarily on the effects of the NMDA antagonist MK-801 and the AChE inhibitor pyridostigmine bromide. We chose MK-801 because it is a prototypical NMDA antagonist and is well-characterized in the *in vitro* brain slice systems with respect to effective concentration and time course of effect. Secondly, MK-801 was used in our parallel *in vitro* studies using patch clamp recordings and in our *in vivo* studies. This will allow us to compare effects across experimental systems.

Also, in these initial studies we have focused on the effects of these drugs in adult female rats. As discussed in our original proposal, adult female animals have been found to be more susceptible to NMDA-antagonist-induced neurotoxicity.

However, for comparison, we have done several preliminary studies using young males. This was important to do, in part, because all previous studies in our lab using this system have been done with young males, so the use of these animals was important to determine the effects of the drugs while using rats of a well-characterized age. In addition, our previous studies have used slices from the hippocampus or amygdala; we did not have experience with slices of the posterior cingulate or retrosplenial cortex. Thus, the use of slices from younger male helped us

compare the responses evoked in the cingulate and retrosplenial gyrus to previously studied anatomical areas. Also, *in vitro* studies with brain slices from adult animals can be difficult, so we wanted to start our study using more hardy (younger) tissue first, to characterize the optimal responses.

In addition, the use of both young and old animals, as well as males and females, is consistent with our initial technical objectives to take age and gender into account in our studies. This is especially important because many experimental studies typically use quite young or peri-adolescent animals (unless they are specifically studying geriatric conditions). This is especially true with *in vitro* electrophysiological studies, because brain slices from young rats (up to early adolescent ages) are much hardier than tissue from adult rats. However, our project is focused on possible toxic risk to which service personnel will be exposed (although we do not rule out exposure to civilians, as well). Accordingly, to correctly "model" people of service age, our animal model should include rats of much older ages than typically used. And this is especially important, because older animals have been shown to be more sensitive to NMDA antagonist-mediated toxicity.

Methods

Pilot Studies:

We have done two sets of experiments: an early set of pilot studies and a more recent set of more formal studies. The latter will serve as the data base for ongoing and future studies.

The early pilot studies were done initially when the photodiode imaging system was being set up in our lab and optimized for recording. In that early system, a high quality, standard vibration isolation table was used. Such tables are very good for most typical electrophysiological studies, but proved to be insufficient for this very sensitive imaging system. (Since those early studies we have added a high-performance vibration isolation table which greatly enhances the quality of the images, so that quantitative results can be obtained.)

Nevertheless, the early images were of sufficient quality to provide a general sense of the drug effects. Accordingly, we want to be clear in stating that the early results were only qualitative in nature. Still, those experiments did provide clues as to what to expect when the system was fully functional using the high-performance vibration isolation table.

Specifically, the pilot studies provided general information about several concentration ranges of drugs and the time course of their effects. In these studies we tested the effect of four NMDA antagonists (MK-801 (10 μM), D-APV (25 & 50 μM), ethanol (40 mM), and ketamine (1, 3 & 10 μM), (an anaesthetic agent with NMDA-antagonist activity)), an AChE inhibitor (pyridostigmine bromide (10 &100 μM), two cholinergic (predominately muscarinic) agonists (carbachol (0.75 μM) and pilocarpine (1 & 10 μM)) and a glutamate agonist (NMDA (10 μM)). The qualitative results from these studies provided early evidence that MK-801 might be excitatory, whereas pyridostigmine might be inhibitory. Based on these results, we focused on these two agents in the more recent experiments. We will use the other agents in future studies.

Recent Studies:

In these studies, we used brain slices from Sprague Dawley rats (Charles River, Raleigh, NC). Two types of rats were used: young males and adult females. These two groups represent the most resistant (young males) and most sensitive (adult females) groups with respect to NMDA-antagonist-induced toxicity. The young males were 28-31 days of age and weighed from 81-104 grams (n=5); rat of this age range are considered early adolescents. The adult female rats used were retired breeders from Charles River. They were delivered to our facility with litters of 14-day-old pups. Their litters were weaned at around 28 days of age, after which time the dams were allowed to recover at least 4 weeks after weaning. During the recovery phase, they were housed 2 to 4 per cage with other retired breeders. The exact age of retired breeders is not provided by Charles River, but they are full-sized adults by the time of use (361-457 grams) (n=4). This assures that we are using animals well within the range that Olney and colleagues have reported as being most sensitive to neurotoxicity.

Rats were anesthetized with halothane and quickly decapitated. The brains were removed carefully to avoid damaging the cortical areas of interest: the posterior cingulate and retrosplenial cortex. Coronal slices (500 μm) were made with a vibratome. Using the hippocampal profile as a guide, slices were selected to include the posterior cingulate and/or retrosplenial cortex, (approximately from -2.3 to -3.8 from the bregma (Paxinos and Watson, 1986)). These slices were further dissected to remove the ventral half of the brain, leaving the hippocampus and overlying cortex intact. (This last step was done so that the large brain slices of the adult females could fit into the recording chamber (designed for much smaller hippocampal slices of young rats) while leaving both sides of the cingulate or retrosplenial cortex intact and connected.) Slices were then incubated in artificial CSF composed of (in mM):NaCl, 124; dextrose, 10; NaHCO3, 2.6; KCl, 2; KH2PO4, 1.25; CaCl, 2; and MgSO4, 1, equilibrated with 95% O2 and 5% CO2.

After 1 hour of incubation, slices were stained in ACSF with the fast voltage-sensitive dye JPW1131 (also known as RH479) (from Dr. L. Loew, University of Connecticut, Farmington, CT) at 0.02 mg/ml for 40 to 60 minutes. The stained slice was then placed in an immersion-type recording chamber and perfused with ACSF at 2-3ml/min and at 29 °C for at least 60 min to stabilize the slice and allow unbound dye to wash out of the slice.

The optical signal was obtained using an upright microscope (Axioskop 2FS; Carl Zeiss, (www.ziess.de) with a water immersion lens (10X) and two camera ports. One camera port was equipped with a fixed zoom lens and a fast CCD camera (SensiCam; Cooke Corp. Ltd., (www. cookecorp.com) for taking pictures of slices and calibrating the objective plane. The other camera port had a changeable zoom lens and a 464-element photodiode array (WuTech Instruments; (www. wutech.com) that covered a 1 mm-sided hexagon area. The fastest sampling rate of the photodiode array is 0.613 ms per frame. Both the CCD camera and the photodiode array were calibrated independently. The double calibration allowed us to correlate a specific spot of the slice to a particular diode. 10 kHz low-pass and 0.2 Hz high pass RC filter were used in the first stage amplifiers. Detailed descriptions were available (see Wu, et al., 1999b). Data acquisition and analysis was performed with the program NeuroPlex (RedShirt Imaging, LLC.,

www.redshirtimaging.com) on a Pentium PC. A vibration isolation system (250WS-1; Minus-k Technology, www.minusk.com) was used to minimize the vibration noise.

A unipolar tungsten microelectrode (.02", 5 MΩ, 8 Degree; A-M System Inc., Carlsborg, WA) placed in the deep layers of the cingulate or retrosplenial cortex to deliver stimulating impulses. The intensity of stimulation was 70-100 μA/200 μs.

After at least 60 min of washing of the stained slice in the recording chamber, a 2-second data acquisition (at a sample rate of 0.613ms per frame) was triggered manually every 4 minutes. The stimulus was delivered during the acquisition with a 0.5 s delay. Averaged responses from a 240 x 240 μm2 area (3 by 3 diodes) close to the stimulating electrode was constantly observed until the responses were stabilized for half an hour before applying any drug. With this method of recording, the responses will remain unchanged for at least 2 hours (Wang, et al., submitted).

Once the controls were stabilized for 30 minutes (8 recordings), the MK-801 was applied for at least 30 minutes, followed by pyridostigmine-plus-MK-801 for 30 minutes. Four recordings from each phase were then averaged for comparison. With the evoked response, the very tip of the stimulating electrode generated an artifact which was revealed by a single diode that had a significantly large response than other diodes. (Responses from all other diodes were physiological as they could be blocked by TTX (Wang, et al, submitted).)

The response of voltage sensitive dye has a submillisecond kinetics and a linear dependence to voltage change within ±100 mV (L. M. Loew, 1999). JPW1131 has a specific light absorption at 705 ± 50 nm. The optical imaging was made of pseudocolor intensity scaling in which the warm color corresponded to depolarization. A fixed scale was used to compare the images between the control and drug application. In this mode, signals from every diode are relative to the fixed scale so that the changes before and after drug can be determined.

All pharmacological agents were obtained from Tocris, Sigma (pilocarpine, pyridostigmine, physostigmine and carbachol), or RBI (D-APV and MK-801).

Results:

As shown in Figure 1, the stimulating electrode is positioned in the deep layers of the retrosplenial cortex (Figure 1A). When a single stimulus pulse was delivered to this area, the signal propagated around the stimulated area (Figure 1B, warm (yellow and orange) colored area). After 3 μM of MK-801 was applied, the spreading area was enlarged and the intensity of depolarization was increased (Figure 1C, red color). Subsequent application of pyridostigmine bromide (100 μM) inhibited both spreading and intensity of depolarization (Figure 1D). Once again, these results are qualitative in nature: extensive quantitative analysis to determine the extent of the increase is ongoing. In general, preliminary measures of the results from adult females suggest that a low concentrations (3 μM) of MK-801 causes a period of depolarization, whereas pyridostigmine (100 μM) was inhibitory. In contrast, MK-801 at much higher

concentrations (40 μM) may be inhibitory in adult females as well as young males. Pyridostigmine (100 μM) also appeared to be inhibitory in the young males, but, again, these results are very preliminary and await detailed quantitative analysis. (Low concentrations of MK-801 have not been tested yet in slices from young male but these concentrations will be tested shortly. Also, we will test the effect of the drugs in adult males and young females to further explore their different vulnerabilities.)

Discussion:

These studies provide preliminary evidence that a dose of MK-801 enhances evoked responses in the cingulate cortex in adult female rats. If this depolarization reflects a sustained depolarization of many neurons, it is possible that the stress of such a response could damage vulnerable neuron populations. If such a difference could expose either excitatory or inhibitory neurons to excitotoxic levels of glutamate or levels of intracellular calcium (or other neurotoxic mechanisms), then certain cells may be permanently lost. These studies also demonstrate that an *in vitro* system may be used to study NMDA antagonist-mediated neurotoxicity.

In addition, an inhibitory effect of pyridostigmine bromide was seen consistently in this system. This result is intriguing, because it suggests that pyridostigmine may be protective against other types of neurotoxicity, in addition to its protective effect against nerve agents like soman.

Other investigators have also found that pyridostigmine enhances inhibition using an *in vitro* system. Santos et al. (2000) used cortical brain slices from rats and human to study the effect of pyridostigmine on evoked GABAergic and glutamatergic post-synaptic currents (IPSCs and EPSC, respectively) in rat hippocampal pyramidal cells. They found that pyridostigmine (30 nM - 1μM) increased the amplitude of the IPSC's, but did not alter the amplitude of EPSCs. They note that these finding suggest that pyridostigmine may facilitate GABAergic transmission. They also note that a different inhibitor of acetylcholinesterase (galanthamine) used in human tissue may also enhance inhibition, but may do so through an action on nicotinic acetylcholine receptors. Thus, pyridostigmine may have several protective mechanism by which it reduces soman neurotoxicity: (1) through its action on acetylcholinesterase and (2) through an enhancement of GABAergic inhibition.

Military Relevance:

Probably one of the most important findings in these studies is that pyridostigmine is inhibitory in this system - at least at the concentrations employed. If this translates into neuroprotection *in vivo* against NMDA antagonists, it may have clinical relevance. For example, this may help explain why pyridostigmine may be protective against soman toxicity. If pyridostigmine gains access to the brain before or during an exposure to an agent such as soman, it may be protective centrally through several mechanisms. However, it is important to stress that these are preliminary results with only one concentration of the drug, and other concentrations (and drug combinations) must be tested to make sure there are not dangerous interactions due to synergy of particular agents or doses.

Furthermore, given the importance in current national policy to reduce the number of

experimental animals used in studies, and to avoid their pain and suffering, this system has definite advantages. For example, this *in vitro* system may have the advantage of reducing the number of animals needed to address specific questions, since several drug concentrations and combinations can be tested on a single slice. In addition, this system greatly limits distress caused to the animals compared to more traditional, long-term *in vivo* studies of toxicity. Furthermore, the results from these studies may be used to help plan *in vivo* studies more wisely, so that, once again, fewer animals may be used in the *in vivo* studies. At present, it is not possible to do without *in vivo* studies altogether, but with careful, rational linking of *in vitro* and *in vitro* animal studies, we hope to be more efficient experimentally. Most important still, is that this system allows hypotheses to be tested in animal models, which, in the long run we hope will reduce the risks to which service men and women are exposed.

Future Aims:

Future aims using this technique will proceed in several directions. First, we will analyze in detailed the results from the recent experiments using adult female and young male rats. We will examine the responses recorded from individual photodiodes to assess the changes in specific anatomical subregions in these slices. In addition, we will also determine the time point at which drug onset occurs: initial qualitative results suggest that MK-801 has a more rapid effect than was expected, but quantitative assessment must be done to test this impression. However, a rapid onset would be consistent the rapid onset of effect seen *in vivo*. It is possible that this system is quite sensitive to certain aspects of drug onset effects. These analyses will also help us pinpoint regions and time points on which to focus in future studies. In addition, as discussed above, we will examine the effect of lower concentrations of pyridostigmine bromide in our system.

Then, we will focus on the following questions:

1. Does low-dose MK-801 (3 μM) have a similar excitatory effect in brain slices from adult male rats, but have less of an effect in young female and young male rats? If there is such a parallel with the *in vivo* findings, then it supports the validity of this system and supports its further use in studying the neurotoxic mechanisms.

2. Is pyridostigmine more effective at inhibiting the effect of MK-801 when it is administered first? This order of administration may more closely model the sequence of administration in certain military settings. For example, if there was a threat of a soman attack, pyridostigmine might be administered daily - then, if the attack occurred and personnel were exposed, a drug with NMDA antagonist activity might be administered to treat the acute symptoms (e.g, either used as a neuroprotective agent or as an anticonvulsant in individuals having soman-induced seizures). Accordingly, to test the effect of order in our system, pyridostigmine will be given first, then MK-801 (or an other NMDA antagonist) will be added to the pyridostigmine-containing solution.

3. Can our findings in this system shed any light on the results from our other experiments using *in vivo* or *in vitro*. Can the patch clamp recording system shed light on which cell type may be causing this depolarizing effect? Can the photodiode images help determine the specific dose ranges at which pyridostigmine is protective *in vivo*?

4. Do other AChE inhibitors have similar inhibitory effect (e.g., physostigmine or galanthamine)

5. Do other NMDA antagonists have similar excitatory effects (e.g., memantine or ethanol).

6. Since we are using the bromide salt of pyridostigmine, we will rule out a possible contribution of bromide to the effect of pyridostigmine.

Figure legends

Figure 1.

Effects of MK801 and pyridostigmine on the evoked depolarization and its propagation in the retrosplenial cortex. **A.** CCD camera image of a section of the slice showing the stimulating electrode in the retrosplenial cortex. **B.** A photodiode image of an averaged evoked response to single stimulus in the deep layer of the retrosplenial cortex in the control condition. The signal spread around the stimulated area. **C.** An averaged response after MK801 (3 μM) was applied. Red color indicates that the depolarization level was increased. The area of signal spreading is larger than that in the control. **D.** An averaged response after subsequently adding pyridostigmine (100 μM) revealed a decrease in the level of depolarization and area of spreading of the evoked signal.

Note: The frames represented the responses at 33 ms after the stimuli were delivered under each condition. This time is within the scope of the highest $GABA_A$ effect. Depolarization was represented by warm color while hyperpolarization was represented by cold color. Fixed scale was used for pseudocolorization in which every response trace was relative to a fixed scale; this technique best revealed the spatial distribution of the signal propagation. The depolarization generally decayed to baseline within about 200 ms. Signal intensity beyond the scale was represented by the limits of the scale, i.e., the red color represents the intensity that great than or equal to the upper limit of the scale.

Figure 2.

Effects of MK801 and pyridostigmine on the evoked depolarization and its propagation in the retrosplenial cortex: a dynamic view.

Pseudocolor frames from photodiode arrays display the intensity of optical signal in the retrosplenial cortex in three different conditions: Control (drug-free) ACSF, MK-801 (3 μM), and MK-801 (3 μM) plus pyridostigmine bromide (100 μM). Stimulations were delivered to the deep layers of the retrosplenial cortex as shown in figure 1.

Each row of 10 frames covered the response from 22.5 to 45 ms after the stimulus. Each successive frame is separated by 2.5 msec. All frames are from the same slice as shown in figure 1. (The three enlarged frames in figure 1 are from a time point between the 4^{th} and 5^{th} image (counting from the left) of each of row).

Figure 3:
Typical brain slice used in photodiode imaging studies. Rectangle shows the approximate location of cortical area on which is focused the CCD camera image (square) and photodiode image (hexagon), as shown in figure 1. Also shown is the ventral area that has been trimmed from the coronal section before placing it in the recording chamber.

References:

Keller A, Yagodin S, Aroniadou-Anderjaska V, Zimmer LA, Ennis M, Sheppard NF, Jr., Shipley MT (1998) Functional organization of rat olfactory bulb glomeruli revealed by optical imaging. J Neurosci 18: 2602-2612.

Laaris N, Carlson GC, Keller A (2000) Thalamic-evoked synaptic interactions in barrel cortex revealed by optical imaging. J Neurosci 20: 1529-1537.

Lowe LM (1999) Potentiometric membrane dyes and imaging membrane potential in single cells. In: *Fluorescent and luminescent probes for biological activity* (Mason WT, ed), pp 210-221. New York: Academic Press.

Paxinos G, and Watson C (1986) The Rat Brain in Stereotaxic Coordinates. Second Edition. San Diego: Academic Press.

Santos MD, Alkondon M, Aracava Y, Eisenberg HM, Maelicke A, Albuquerque EX (2000) Effects of pyridostigmine and galanthamine on synaptic transmission in the mammalian central nervous system. Neurosci. Abst., 26:1914.

Tsau Y, Guan L, Wu JY (1999) Epileptiform activity can be initiated in various neocortical layers: an optical imaging study. Journal of Neurophysiol. 82: 1965-1973.

Wang, C J, Wilson, WA & Moore, SD, Evoked responses in the amygdala complex revealed by optical imaging coupled with a voltage-sensitive dye. *Submitted.*

Wu J-Y, Cohen LB, Falk CX (1999b) Fast multisite optical measurement of membrane potential: with two examples. In: *Fluorescent and luminescent probes for biological activity* (Mason WT, ed), pp 222-237. New York: Academic Press.

Wu J-Y, Guan L, Tsau Y (1999a) Propagating activation during oscillations and evoked responses in neocortical slices. J Neurosci 19: 5005-5015.

FIGURE-1

A

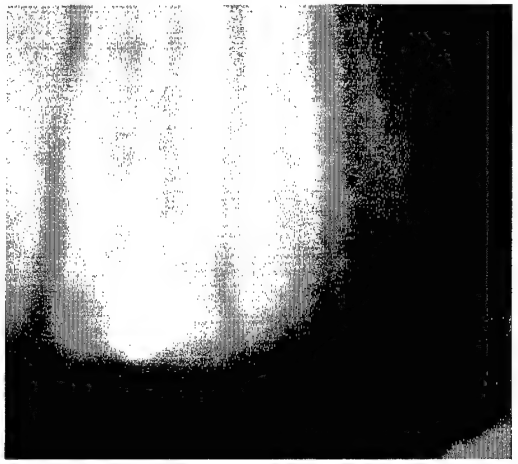

The stimulating electrode
in the retrosplenial cortex

B

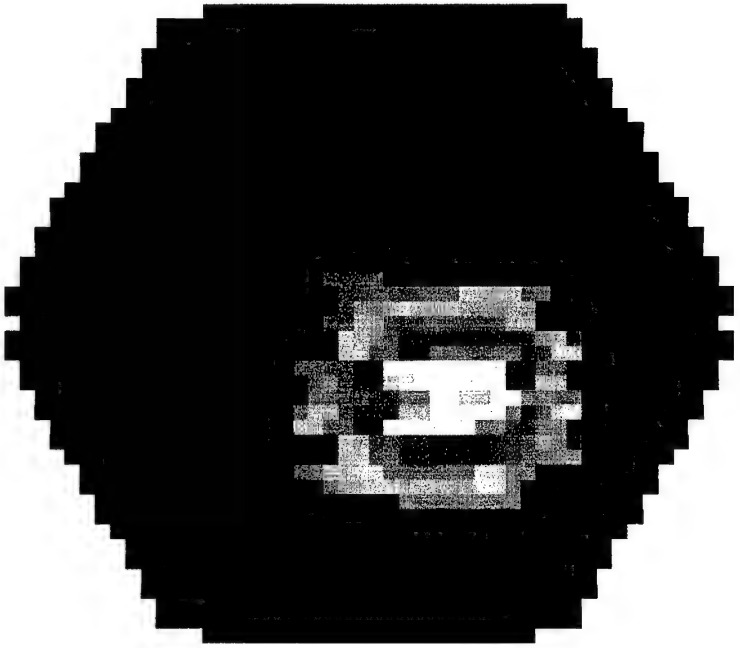

Control

C

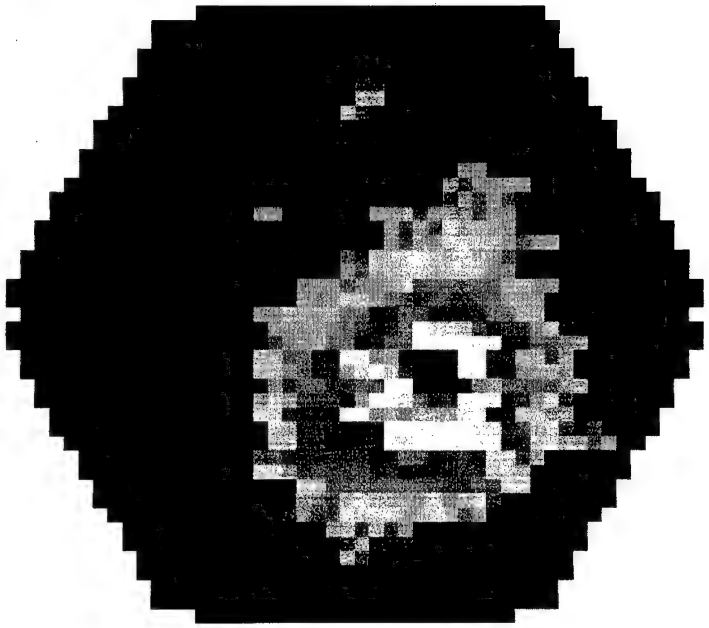

MK801

D

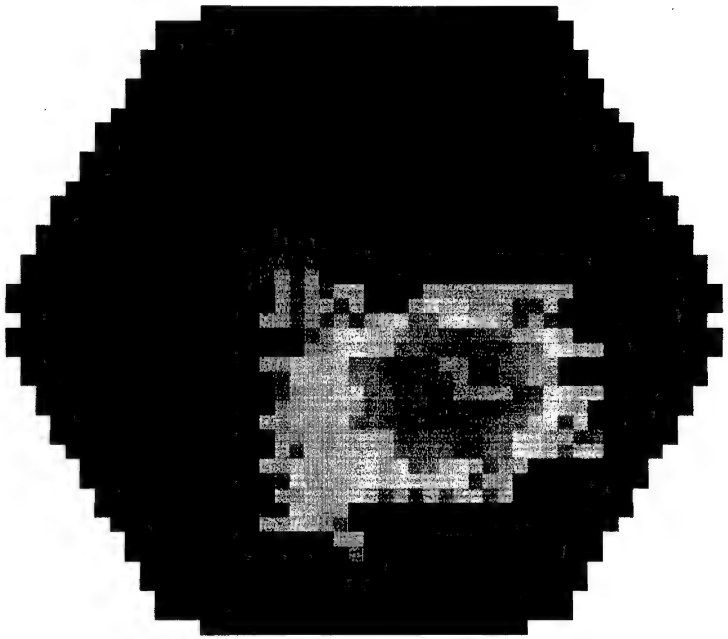

MK801 + Pyridostigmine bromide

FIGURE-2

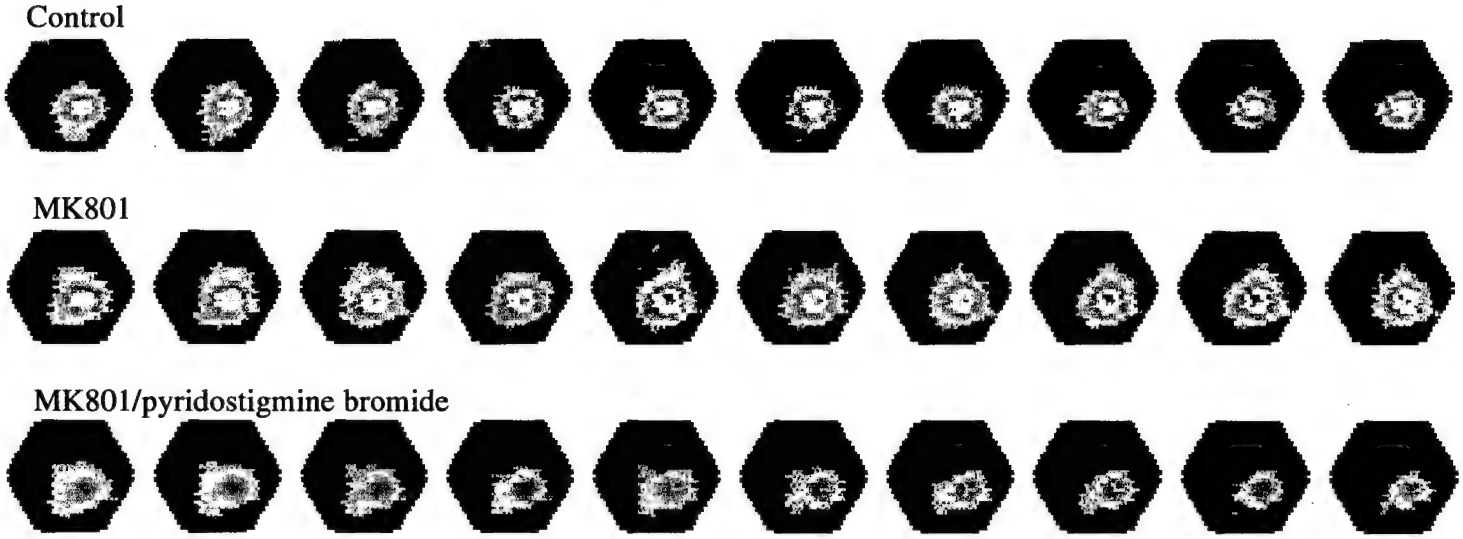

FIGURE-3

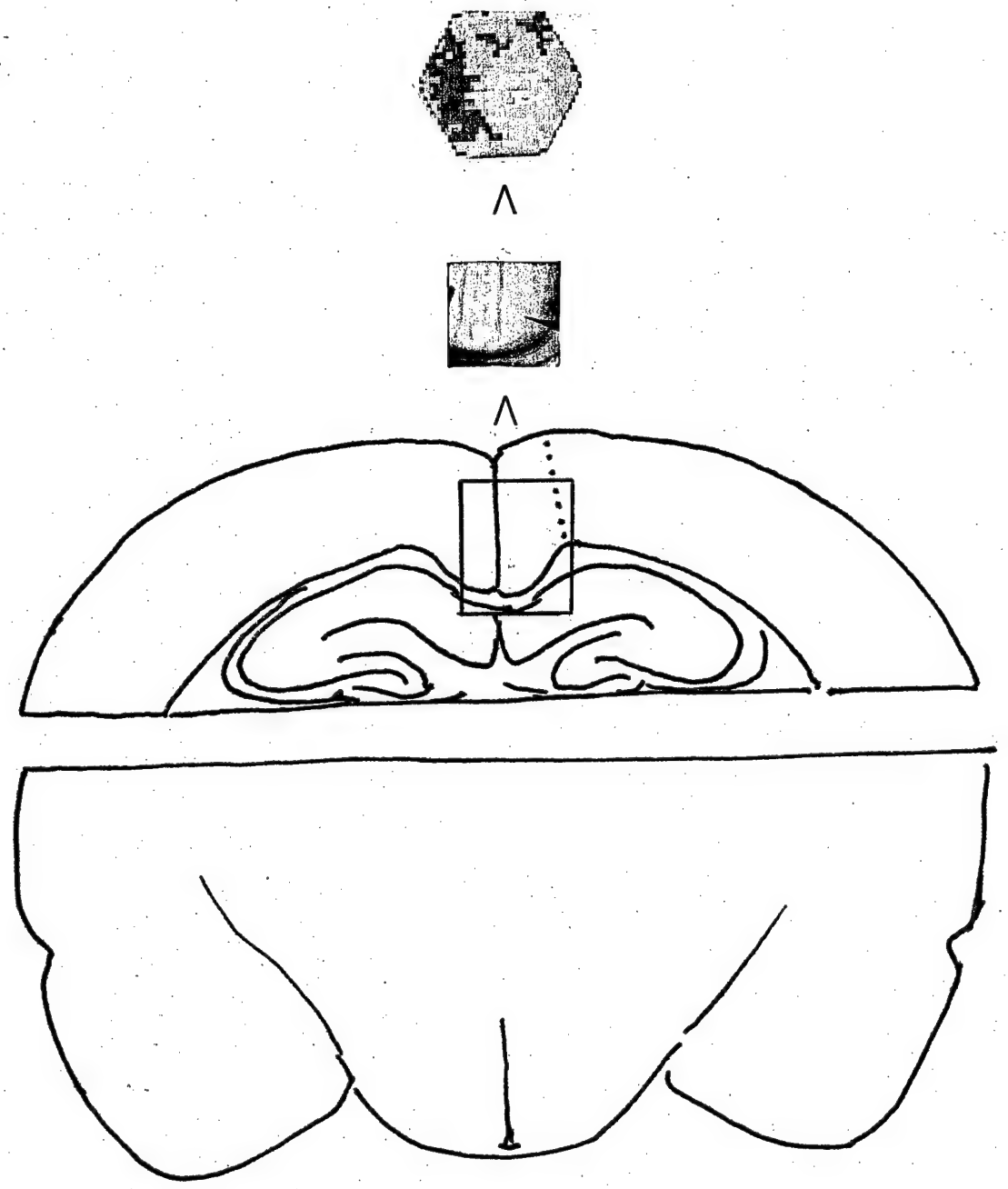

Using Fluoro-Jade Staining to Measure Interactions between NMDA Antagonists and Acetylcholinesterase Inhibitors in the Rat Cingulate Gyrus and Retrosplenial Cortex

Introduction

Discussed here are preliminary findings from histological and behavioral studies that evaluate potential neurotoxic interactions between: (1) antagonists of the *N*-methyl-D-aspartate receptor/channel complex (NMDA r/c antagonists) and (2) acetylcholinesterase inhibitors (AChEIs).

It is important to explore the risks associates with combinations of these agents, because if these two types of agents act synergistically to enhance (or reduce) neurotoxicity, it will be of military and civilian importance. First, these types of agents are widely used: AChEIs are common in the military environment, including their use as insecticides and as protective agents against chemical warfare agents such as soman. Although less common, drugs with NMDA-antagonist activity are available, and many new ones are being developed. Indeed, drugs with some degree of NMDA-antagonist activity that are on the market or in clinical trials include anticonvulsants (felbamate (Rho, Donevan & Rogowski, 1994)), antitussives (dextromethorphan (Britton, et al, 1997)), anti-Parkinson's agents (memantine (Kornhuber and Weller, 1996)), and recreational drugs (ethanol (Lovinger, 1989; Ikonomidou, et al., 2000)). It is probable that this list will only increase in length, because NMDA antagonists have been the focus of new therapies for chronic pain, as well as seizures caused by chemical warfare agents (e.g., see Filliat, et al., 1999). Thus, in the future it is likely that some military personnel and civilians will be exposed concomitantly to AChEIs and NMDA antagonists.

The neurotoxicity of NMDA antagonists actually came as a surprise, for it was originally hoped these drugs would be neuroprotective (Rothman and Olney, 1995). This unexpected neurotoxicity was characterized in a series of papers by Dr. John Olney and colleagues (see review by Olney, 1994). Olney first reported that non-competitive NMDA antagonists produce vacuoles in neurons of the posterior cingulate (PC) and retrosplenial cortex (RSC) within four hours of exposure, but the effect appeared to be reversible (Olney, et. al., 1989). This reversibility suggested that neurons would recover eventually. Then, in 1991 they reported that higher doses of NMDA antagonists could produce

permanent neurodegeneration (Olney, et al., 1991). The seriousness of this effect is new well-recognized, and has been reproduced elsewhere (Auer, 1994; Ellison, 1995; Hargeaves, et. al, 1993; Schmued, et al, 1997; Schmued & Hopkins, 2000).

Many neurotransmitter systems modulate NMDA antagonist-induced neuronal degeneration. It can be blocked by atropine (a muscarinic cholinergic antagonist), suggesting that cholinergic processes modulate NMDA antagonist-mediated neurotoxicity (Olney, 1991). Barbiturates and benzodiazepines were also protective (Olney, 1991), as were alpha-2 adrenergic agonists (Farber, et al., 1995) and antipsychotics (Farber, et al., 1996; Sharp, et al., 1993; 1994). Later, dramatic evidence of cholinergic modulation came from a study showing that NMDA antagonist-induced neurotoxicity could be greatly increased by co-administration of pilocarpine, a muscarinic agonist (Corso, et al., 1997).

Although the effect of pilocarpine is instructive with respect to the toxic mechanisms, it may have limited clinical relevance with respect to CNS damage, since only a few drug are available that are direct agonists of central muscarinic cholinergic receptors (e.g., pilocarpine drops for glaucoma). However, this finding argued for investigations of other cholinergic modulators, including AChEIs. The AChEIs are used widely as insecticides (e.g., the organophosphates) and drugs (e.g., tacrine for Alzheimer's disease (Taylor, 1998)). Furthermore, given the risks chemical warfare attacks, it is probable that military use of AChEIs may still be necessary, based on studies showing their effectiveness against such exposures (Leadbeater, 1985; Phillippens, et al., 1996). In addition, some AChEIs are highly potent or have a long duration of action, such that even low levels of AChEIs might be problematic when co-administered with NMDA antagonists. Given the risk that both types of agents will be co-administered, we began the following studies.

Methods:

Rats were housed in the Durham Veterans Administration Vivarium under the care of Dr. Gerald Olsen, kept on a 12 hour light and dark cycle, and allowed access to food and water. All efforts were made to reduce animal stress and suffering, in accordance with the *Guide for the Care and Use of Laboratory Animals* (1996) and the current *Durham VA Medical Center Manual for Animal Research,* and all efforts were made to reduce the number of animals needed, while maintaining statistical

validity.

As discussed in the technical objectives, our methods were similar to those used by Olney and colleagues with respect to rats (age and gender), drug doses (MK-801), and behavioral observations (Olney, et al., 1991; Corso, et al., 1997). We used Sprague Dawley (S-D) rats from Charles River (Raleigh, NC). Most were adult females; a few young males were used (36 days of age). (These two groups represent the most sensitive (adult females) and most resistant (young males) groups with respect to NMDA-antagonist-induced toxicity.) The adult female rats were retired breeders delivered to our facility with litters of 14-day-old pups. Litters were weaned at ~ 28 days of age, after which time the dams recovered at least 4 weeks. The exact age of retired breeders is not provided by Charles River, but the rats are full-sized adults when used (300-500 g). This assures that we are have animals well within the range reported as being most sensitive to neurotoxicity.

Rats were randomly assigned to a control or treatment group. Rat were weighed before experiments, then given drugs (or vehicle), intra-peritoneal (ip) or subcutaneous (sc), in a volume of 1ml/kg. In rats given 2 different drugs, MK-801 was given first, after which the AChEI was given within 5 minutes. Drugs were prepared fresh each day and dissolved in sterile saline for injection. The (-) physostigmine sulfate and pilocarpine HCl were protected from light; (-) physostigmine sulfate was checked for light-induced degradation (red color).

The following drug doses were given: (+)MK-801 (0.3-5 mg/kg); (-) physostigmine sulfate (0.03-1.0 mg/kg), and pyridostigmine bromide (0.1 mg/kg). The higher doses of MK-801 were given when we were developing the Fluoro-Jade staining technique. This was to assure we would have many positive cells for staining. (The ED_{50} for producing vacuoles detectable by light microscopy PS/RSG cortices in adult female S-D rats was (0.18 mg/kg sc) (Olney, et al., 1989); higher doses (5.0 mg/kg sc) produce severe vacuole reaction in the cingulate and R/S cortex (Olney, et al., 1991).)

After injections, each rat was placed in a clear plastic cage and observed for drug-induced changes in behavior at hourly intervals. The severity of three behavioral effects (ataxia, hyperlocomotion, and head weaving) were be scored on a scale of 1-3 (for ataxia) or 1-3 (for head weaving) (Hönack & Löscher, 1993; Löscher & Hönack, 1991) and duration of recumbancy. Since

agents which increase cholinergic drive can produce severe seizures at high doses (Turski, et al., 1989), rats were monitored for behavioral evidence of status epilepticus (continuous rapidly recurring seizures), because, on their own, such seizures can cause neuronal death or damage. This has not happened yet, but any rat found in status epilepticus will be euthanized. Dosing was adjusted if necessary (e.g., when too high given in combination).

Perfusion and Histopathology:

After 3 days, rats were anesthetized with Halothane and transcardially perfused with heparinized saline followed by 4% paraformaldehyde. Brains were removed immediately and post-fixed overnight or, in some cases the perfused rat was refrigerated overnight and the brain removed the next morning. (The latter was suggested by R. S. Sloviter for vibratome, next-day sectioning). Brains were transferred to 0.1 M phosphate buffer (PB) for one day, then to 30% sucrose for 3 to 4 days, until they sink. Cryostat sections were cut (40 μm), then stored in 0.1 M PB at 4° C. Sections were processed for Fluoro-Jade staining as described (Schmued, et al. 1997). Sections were mounting in distilled water on gelatinized slides, dried over night, and processed in the following solutions: 100% EtOH (3 min); 70% EtOH (1 min); distilled water (1 min); 0.06% potassium permanganate (7.5 min with slow shaking); distilled water (1 min); 0.001% Fluoro-Jade working solution (30 min with slow shaking in the dark); distilled water (3 times for 1 min), then dried in dark for at least 2 hours (but ≤2 days), dehydrated in alcohol and xylene, then coverslipped with D.P.X., Sections were examined with an epifluorescence microscope using a FITC filter. Assessment of neurotoxicity was performed by an individual blinded to treatment. Bilateral cell counts were made from 4 sections from the posterior cingulate and 4 from the retrosplenial cortices (Figure 1). On occasion, slides from other levels (and other brain areas) were examined for any additional or unusual changes. From Sigma/RBI (St. Louis, MO) we obtained (+)MK-801, (+)pilocarpine HCl, pyridostigmine bromide, (-) physostigmine sulfate; chemicals were from Sigma or Mallinckrodt. Fluoro-Jade was obtained from Histo-Chem, Inc. (Jefferson, AR).

Results:

Initially, pilot studies using high-dose MK-801 were done to facilitate development of the

Fluoro-Jade staining method, which was new to our lab and area. Several months were required to reach a point at which reproducibly good perfusions and staining occurred. A well-stained slide has low background staining (pale green) on which the Fluoro-Jade positive cells appear as bright yellow-green cell bodies and processes. These are relatively easy to count; we have good agreement between individuals counters. Initially we tried vibratome-cut sections, which have the advantage of eliminating the 4 days of post-perfusion processing, but found the sections inferior to cryostat-cut sections.

Our initial experiments involved dose-finding studies to determine tolerable concentrations of physostigmine and MK-801. Originally we had chosen physostigmine because it is widely used experimentally and has been proposed for use against chemical warfare agents (Phillippens, 1996), since it gains access to the CNS, and may give better protection than pyridostigmine (which does not as readily cross the blood brain barrier). Unfortunately, two rats died when given physostigmine (1 mg/kg or 0.3 mg/kg) in combination with MK-801 (3 mg/kg). The rats that got either drug alone (either 0.3 mg/kg physostigmine or MK-801 3.0 mg/kg) survived. This suggests that the combination is synergistic, although the numbers are far too small to draw conclusions; more experiments at lower doses are needed.

However, in parallel to the physostigmine study, we were testing pyridostigmine bromide. This AChEI was chosen in part because there are many circumstances in which members of the military have been - and could be - exposed to this agent. Specifically, pyridostigmine, was administered as a prophylactic agent in the Persian Gulf War when there was danger of exposure to soman (Golomb, 1999). Although pyridostigmine does not normally cross the blood-brain barrier, it may well do so under conditions in which the blood brain barrier is compromised, such as extreme stress (Friedman, et al., 1996). Thus, it might reach the brain, where it can interact with centrally-active NMDA antagonists. Accordingly, pyridostigmine was a reasonable alternative to phyosostigmine.

The pyridostigmine dose was 0.1 mg/kg. This moderately low dose has been used in rats (Domino, 1987) and also in guinea pigs (Berry and Davies, 1970), the latter in which it was found to be a "maximum sign-free dose". We specifically wanted to use modest doses of pyridostigmine and MK-801, because we want to "model" a clinically reasonable scenario. For example, most individuals who

take clinically effective doses of pyridostigmine do not have serious symptoms (although symptoms may have been higher in Persian Gulf War personnel who took pyridostigmine, and its role in their illnesses has not been ruled out (Golomb, 1999)). For this reason, we chose animal doses that were similarly mild. At this dose, either alone or in combination with MK-801, pyridostigmine was not lethal and, for the must part, well-tolerated (some animals did have transient drooling, but in some rats behavioral symptoms (e.g., head weaving) may have been less severe in the presence of MK-801 (however, often it was difficult to quantify the severity of head weaving.). All doses of MK-801 were tolerated and did not need to be adjusted.

As shown in Figure 2A, in adult female rats, saline-treated rats did not have Fluoro-Jade positive stained cells in the PC/RSC (n=9). Similarly, sections from rats treated with pyridostigmine alone were almost uniformly negative (n=8) (Figure 2B). In contrast, a high dose of MK-801 (3 mg/kg) produced positive staining throughout the PC/RSC. Although in some individual rats, pyridostigmine did not seem to alter MK-801 toxicity, (Figure 4), in one study, positive-staining produced by a low dose of MK-801 (0.3 mg/kg) appeared to be reduced by pyridostigmine (0.1 mg/kg) (n=4) compared to MK-801 alone (n=4), but more studies need to be done to establish significance, because of the response variability. As reported by others, young male rats (P36) were more resistant: no positive cells were seen after a 1 mg/kg dose of MK-801, or after this dose in combination with pyridostigmine (0.1 mg/kg).

We also tried a glial stain (GFAP) on the extra brain sections that were not needed for Fluoro-Jade studies, but have yet to get good results with that method. However, it might be appropriate if we wanted to assess neurotoxicity at time points later than 3 days post-exposure.

Discussion:

Fluoro-Jade staining has proven to be superior to vacuole detection for several reasons. First of all, Fluoro-Jade is not prone to false positives, nor did we find any false positive sections in any of our control (saline-injected) rats. This is consistent with other reports (Schmued and Hopkins, 2000). In addition, Fluoro-Jade staining detects neurons that are degenerating; it appears to stain degenerating cells similarly to the more difficult sliver degeneration stains (Schmued and Hopkins, 2000). Thus,

Fluoro-Jade may be staining cells that will ultimately die. For this reason, we have chosen to use Fluoro-Jade over the method of counting vacuoles, for it may be a better measure of toxicity.

For example, not all vacuole-containing neurons are destined to die. Olney et al., (1991) reported that, after single, moderate doses of some NMDA antagonists - the acute vacuole reaction was reversible, because neuronal degeneration was not detected at later time points. After high (or repeated) doses of NMDA antagonists, vacuolization does appear to be a sign of significant damage in some cells, because some neurons in these areas do become necrotic when examined at later time points using other methods (Olney, et. al, 1991). Since our primary interest is a drug-drug interactions capable of producing chronic or permanent CNS problems (and, since these are more likely to be produced by permanent neurodegeneration) Fluoro-Jade, again, seems to be a superior method.

We have focused initially on the posterior cingulate and retrosplenial cortecies, because these areas are the most sensitive with respect to NMDA antagonist-induced neurotoxicity, but we can also examine other anatomical areas in our sections, in case different combinations of drugs cause additional damage in other areas. Still, since the posterior cingulate cortex is involved in spacial orientation, memory, and movement monitoring (Vogt, 1992), this is an important area to monitor. Given that memory problems are common complaints of ill Persian Gulf War Veterans (Joseph, 1997), and the anatomical basis of these problems have not been elucidated, we should not rule out a role for cingulate damage in such conditions. (Although, of course, many other anatomical areas (e.g., the hippocampus) subserve memory functions in humans, and those areas also can be monitored in our sections.)

There are several interesting pharmacological issues here. For example, if pyridostigmine (or similar compounds) are uniquely protective against NMDA antagonist-neurotoxicity, then it may be a useful agent to take prophylactially, especially if the more centrally-active AChEIs are not protective. However, if it cannot cross the blood-brain barrier, how is it protecting the cingulate? This question, and others, we hope to address in additional studies.

Military Significance:

The health consequences of this study for the military may be quite significant (Horn, et al.,

1997). Given that CEIs can be valuable agents (e.g., as insecticides in areas of insect-borne diseases) or that exposure to them may be unavoidable (as in military or terrorist attacks) it is important to identify potentially dangerous interactions with commonly used agents. Accordingly, if we find that a particular combination of AChEIs and NMDA antagonists is neurotoxic, then a concerted effort can be made to alert physicians, the military and the public of the risks of combined use. However, a parallel issue is equally important: if certain drug combinations appear to be *tolerated*, then there will be no reason to avoid using these agents together. This is important, because for some of these uses (e.g., neuroprotection against soman), there are few other alternatives. We should be reluctant to deprive individuals, whether military or civilian, of the therapeutic benefits of drugs and insecticides (either alone or used in combinations), given the risks they face if such therapies are made unavailable.

Future Studies:

In future studies, we will test additional doses of pyridostigmine to determine if higher (or lower) doses can facilitate MK-801-induced neurotoxicity. In some experiments we will alter the order of dosing: pyridostigmine will be given first, followed in 15 minutes by the MK-801. (Based on our results from the photodiode experiments, the depolarizing effect occurs very quickly after MK-801 is applied to a slice; it is possible that if the pyridostigmine is present when this early depolarization is taking place, that there is more chance for neurotoxicity to occur.) In addition, we will re-evaluate the physostigmine doses, then resume those studies. Then, as proposed, we will test other NMDA antagonists, including drugs most likely to be encountered clinically: memantine (25, 50, and 75 mg/kg), felbamate (100, 300, 400 mg/kg), and dextromethorphan (10, 20 and 50 mg/kg). Later studies will involve experimental agents, such as the non-competitive antagonists, as well as antagonists of the strychnine-insensitive glycine site on the NMDA, some of which may pose less of a neurotoxic risk (Koek & Colpaert, 1990; Auer, 1997; Hawkinson, et al, 1997; Tomitaka, et.al, 1996)) than the NMDA channel blockers (e.g., see Berger, et al., 1994).

Figure 1.

Coronal section of an adult female rat brain section. **TOP:** The region of a Fluoro-Jade stained rat brain section; this photograph was taken using light microscopy to show anatomical details less evident in the other photographs. This view at 10X magnification is representative of the areas of interest in this study (posterior cingulate and retrosplenial cortecies). Perfusion-fixed brain tissue was cut using a cryostat (40 μm). The brown and orange coloration is due to potassium permanganate staining. (calibration bar = 32 μm) **Bottom:** Drawing representing a coronal rat brain section that includes retrosplenial cortex (-3.3 to the bregma). The boxed area approximates the region that was used to quantify Fluoro-Jade staining in the treatment groups.

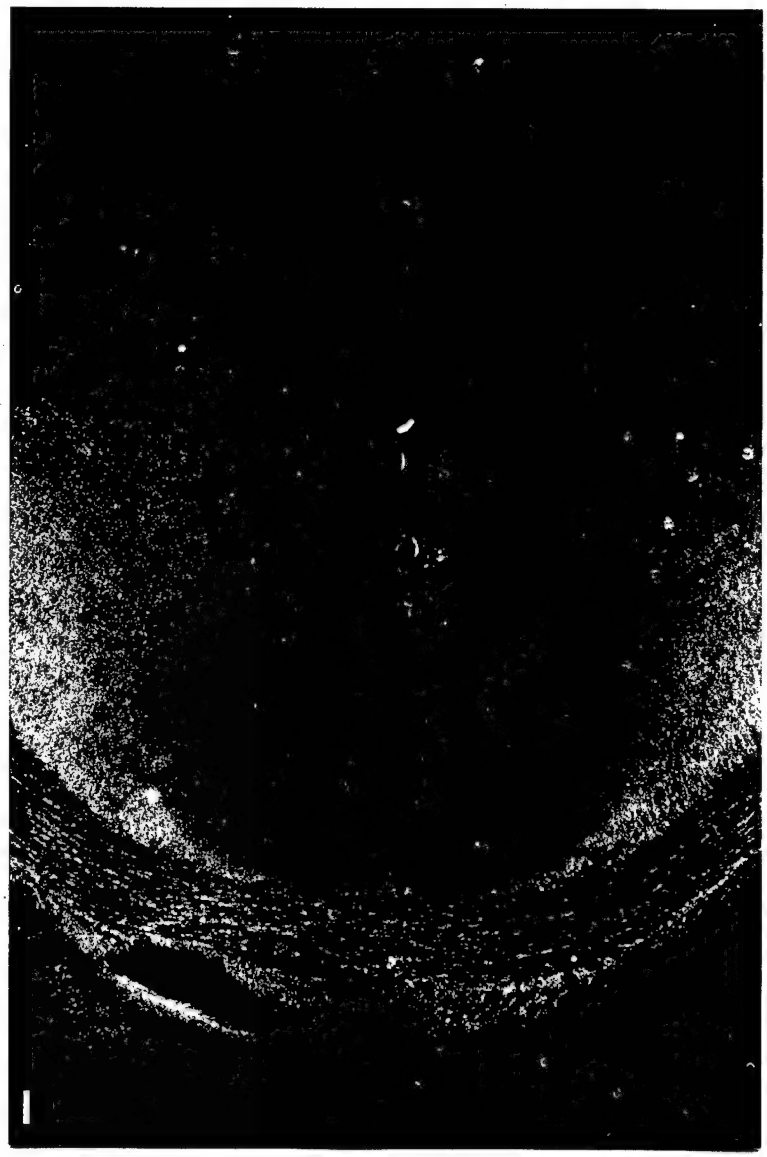

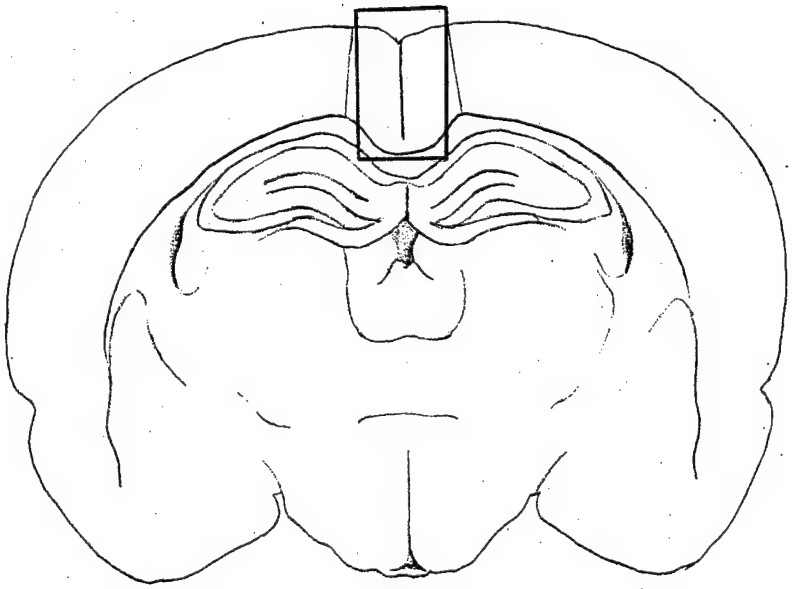

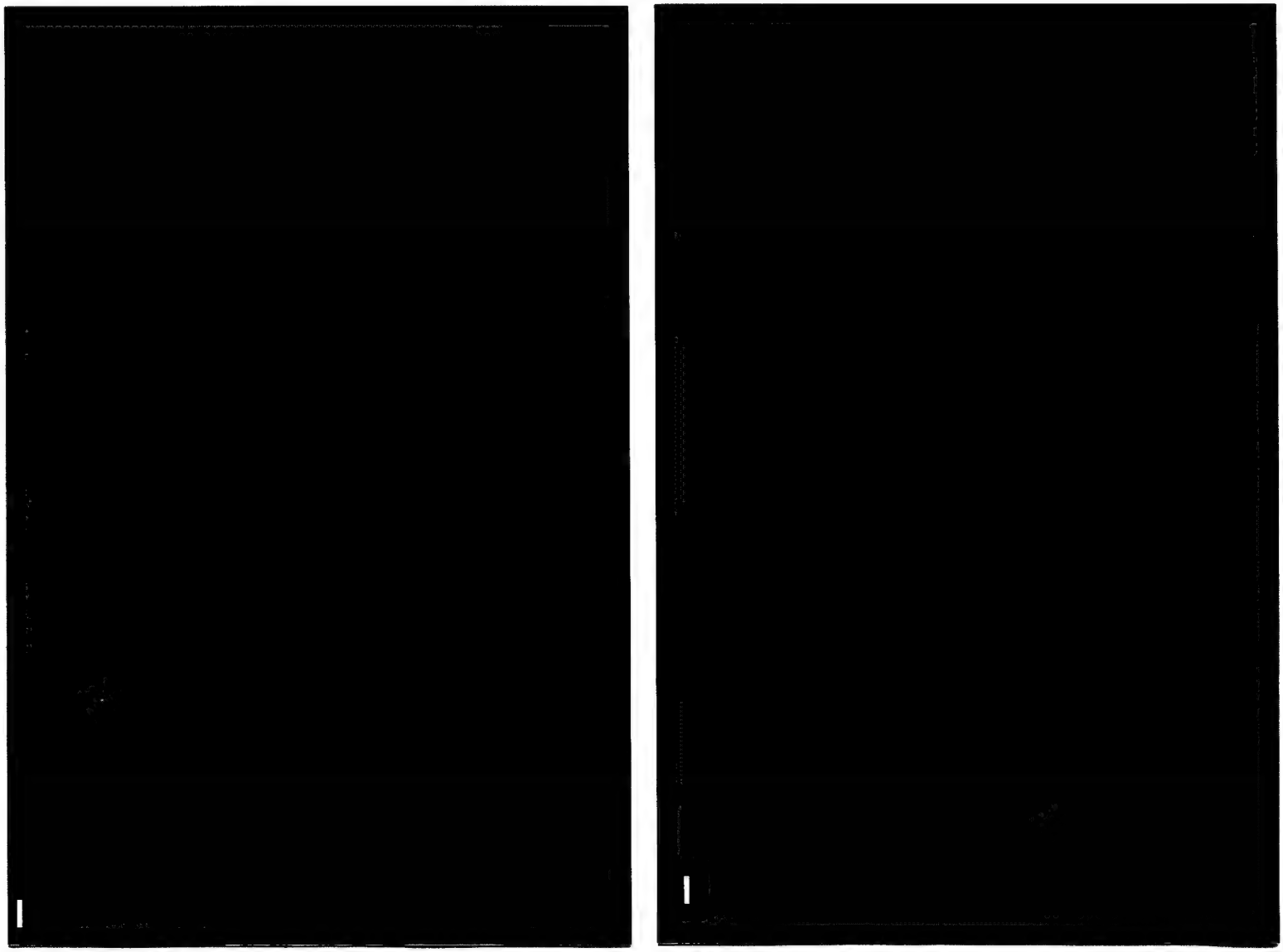

A B

Figure 2. Fluoro-Jade staining of a coronal brain section showing the posterior cingulate region of an adult female rat. Fixed brains were cut with a cryostat (40 μm) and stained. The sagittal sinus is oriented vertically in this image and is located on the left side of each photograph. Three days following treatment with saline or pyridostigmine bromide, no neurodegeneration is evident. Note in both photographs the wide band of lightly staining cells (running vertically along the center). These are lightly staining cells Fluoro-Jade negative (i.e., healthy cells) in layer II. Both photographs were taken at 20X magnification; the bars on each photograph correspond to 16 μm. **A.** Control animals were injected with 0.9% saline s.c. (1ml/kg). **B.** Rats exposed to pyridostigmine bromide were given sc injections at a concentration of 0.1mg/kg (in a volume of 1 ml/kg).

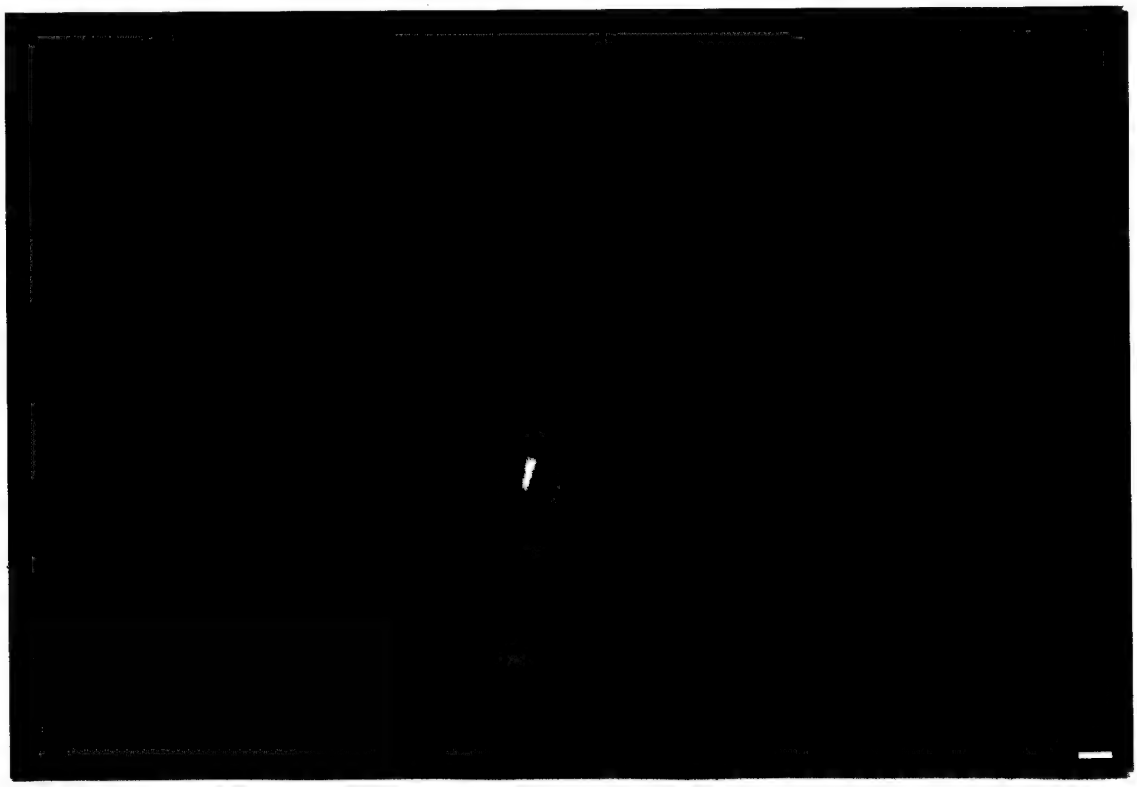

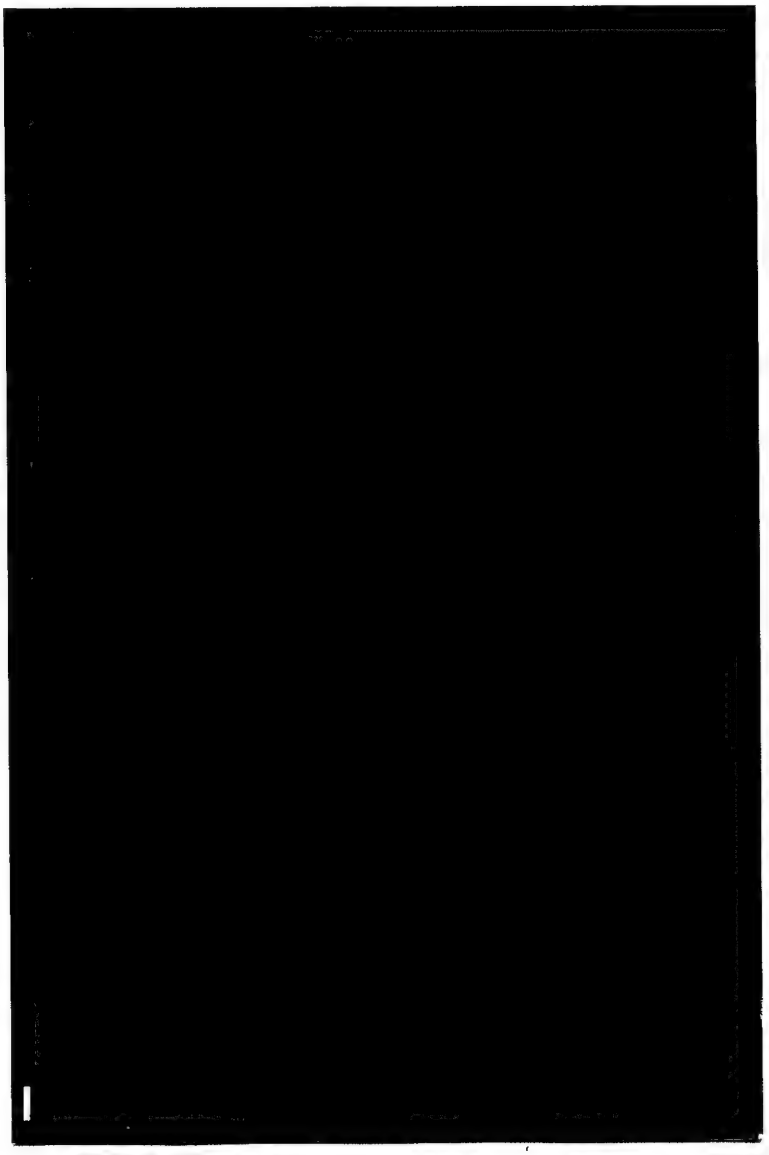

Figure 3.

Fluoro-Jade staining of coronal brain sections of PC/RSC region from an adult female rat that was sacrificed three days following exposure to high-dose MK-801 (3.0mg/kg, sc). Bright yellow cells are Fluoro-Jade positive degenerating neurons; lightly stained cells are not degenerating. **A.** A survey of the cingulate region at 10X magnification demonstrates extensive neurodegeneration on either side of the sagittal sinus. (Calibration bar = 32μm). **B.** A 20X magnification of the right side of photograph in A. (Calibration bar = 16μm). The sagittal sinus is vertically oriented to the left of the photograph.

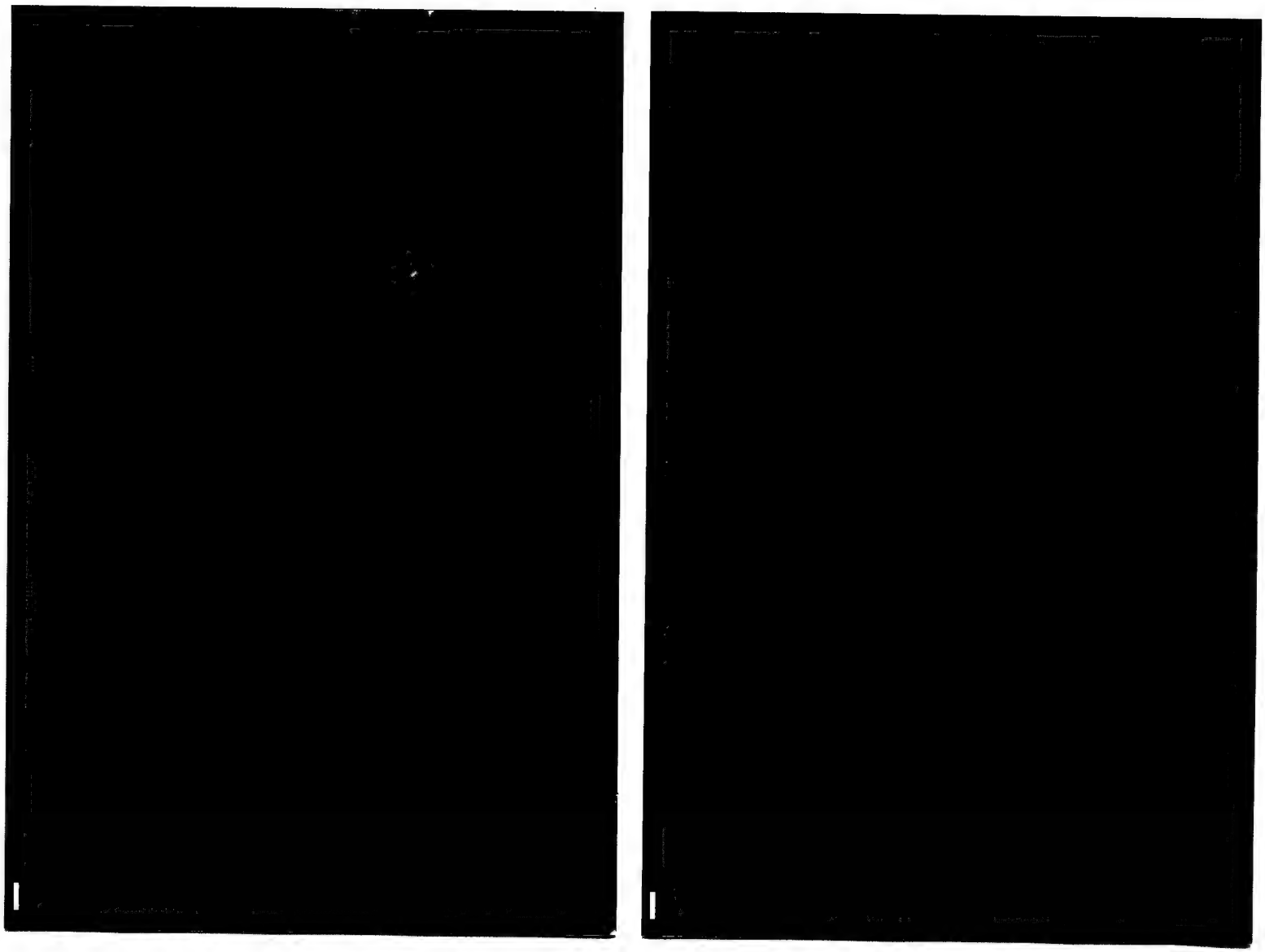

A **B**

Figure 4.

Fluoro-Jade staining of the PC/RSG region in a coronal section from an adult female rat exposed to MK-801 and pyridostigmine bromide. Three days following exposure to MK-801 (0.3mg/kg sc) and pyridostigmine bromide at (0.1mg/kg sc), the rat was sacrificed, perfusion-fixed; coronal sections were cut at 40μm with a cryostat and stained with Fluoro-Jade. The sagittal sinus is oriented to the top in each photograph. Bright-yellow Fluoro-Jade positive cells are clearly evident. **A.** A 20X magnification exhibits both the lightly staining cells in layer II as well as the strong Fluoro-Jade positive cells in layer III. (Calibration bar = 16 μm). **B.** A 40X magnification reveals the morphology of positive staining cells in the deeper layers. (Calibration bar = 8.0 μm).

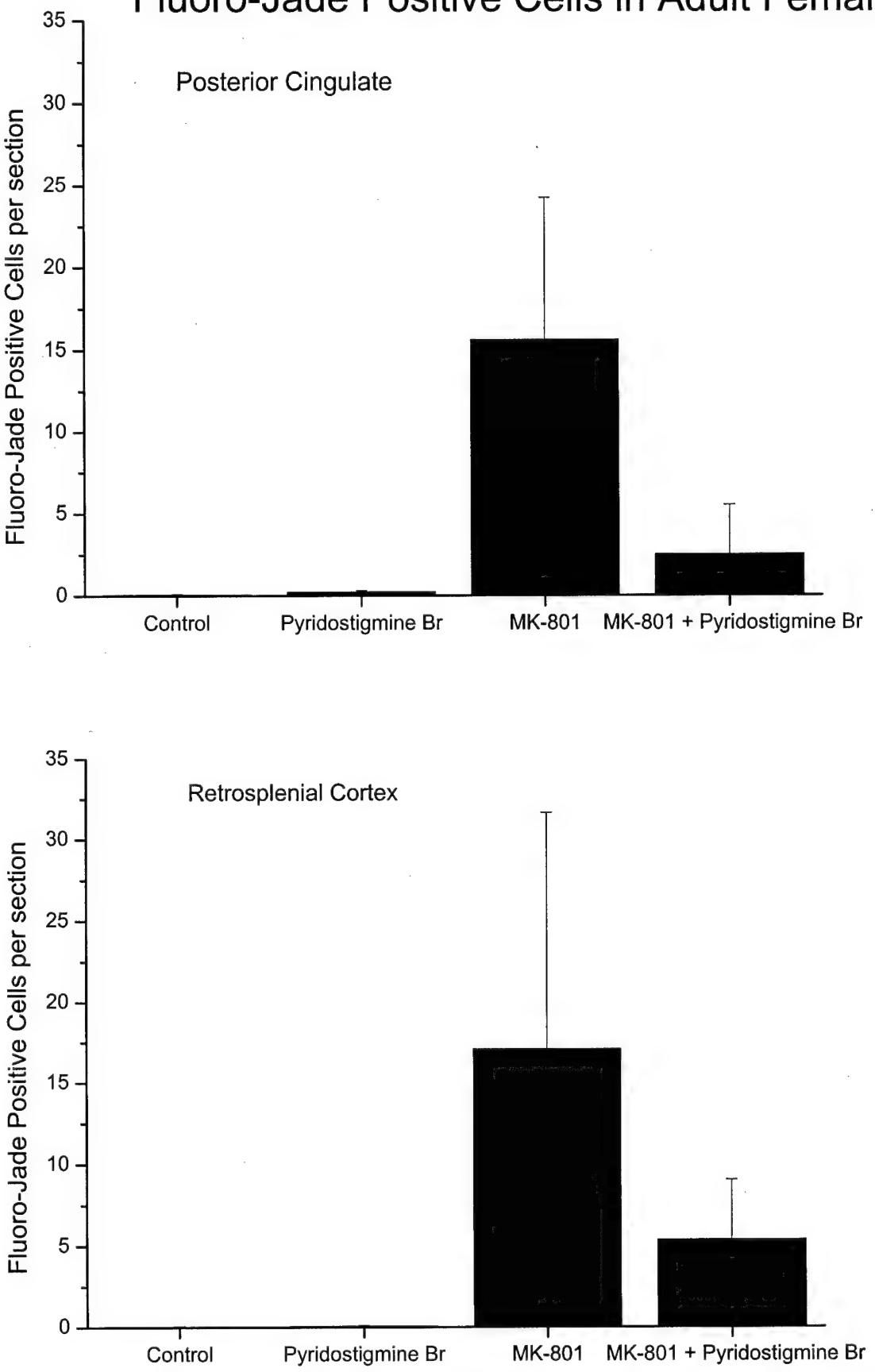

Figure 5: Fluoro-Jade Positive Cells in the Posterior Cingulate and Retrosplenial Cortecies of adult females rats. Rats were treated with s.c doses of saline (Control), pyridostigmine (0.1mg/kg), MK-801 (0.3mg/kg), or both pyridostigmine (0.1 mg/kg) plus MK-801 (0.3 mg/kg). Bars plot average number of cells/section +/- SEM.

References

Auer, R.N., Assessing structural changes in the brain to evaluate neurotoxicological effects of NMDA receptor antagonists. *Psychopharmacol. Bull.* 1994;30:585-591.

Auer R.N., Structural neurotoxicologic investigation of the glycine antagonist 5-nitro-6,7-dichloroquinoxalinedione (ACEA-1021). *Neurotoxicology*. 1997;18:53-62.

Berger, P., Farrel, K., Sharp, F., Skolnick, P., Drugs acting at the strychnine-insensitive glycine receptor do not induce HSP-70 protein in the cingulate cortex. Neurosci. Lett. 1994;168:147-150.

Berry and Davies, *Biochemical Pharmacol.* 1970;19:927-934.

Britton, P., Lu, X.C., Laskosky, M.S., Tortella, F.C., Dextromethorphan protects against cerebral injury following transient, but not permanent, focal ischemia in rats. *Life Sciences* 1997;60:1729-1740.

Corso, T.D., Sesma, M.A., Tenkova, T.I., Der, T.C., Wozniak, D.F., Farber, N.B., Olney, J.W., Multifocal brain damage induced by phencyclidine is augmented by pilocarpine. *Brain Res.* 1997;752:1-14.

Domino, E.F., *Neurotoxicology*, 1987; 8:113-122.

Ellison, G., The *N*-methyl-D-aspartate antagonists phencyclidine, ketamine and dizocilpine as both behavioral and anatomical models of the dementias. *Brain Res. Rev.* 1995;20:250-267.

Farber N.B., Foster J. Duhan N.L., and Olney J.W., Alpha-2 adrenergic agonists prevent MK-801 neurotoxicity. *Neuropsychopharmacol.* 1995;12:347-9.

Farber NB. Foster J. Duhan NL. Olney JW., Olanzapine and fluperlapine mimic clozapine in preventing MK-801 neurotoxicity. *Schizophrenia Res.* 1996;21:33-7.

Filliat, P., Baubichon, D., Burckhart, M-F., Pernot-Marino, I., Foquin, A., Masqueliez, C., Perrichon, C., Carpentier, P., Lallement, G., Memory impairment after soman intoxication in rat: correlation withcentral neuropatholgoy. Improvements with anticholinergic and antiglutamatergic therapeutics. NeuroToxicology 1999;20:535-550.

Friedman A., Kaufer D., Shemer J,. Hendler I,. Soreq H,. Tur-Kaspa I. Pyridostigmine brain penetration under stress enhances neuronal excitability and induces early immediate transcriptional response. Nature Medicine. 2(12):1382-5, 1996.

Golomb, B.A., A review of the scientific literature as it pertains to Gulf War Illness: Volume 2: Pyridostigmine. Rand, 1999.

Hargreaves R.J., Rigby M., Smith D., and Hill RG., Lack of effect of L-687,414 ((+)-cis-4-methyl-HA-966), an NMDA receptor antagonist acting at the glycine site, on cerebral glucose metabolism and cortical neuronal morphology. *Brit. J. Pharmacol.* 1993a;110:36-42.

Hawkinson, J.E., Huber, K.R., Sahota, P.S., Hsu, H.H., Weber, E., Whitehouse, M.J., The *N*-methyl-D-aspartate (NMDA) receptor glycine site antagonist ACEA 1021 does not produce pathological changes in rat brain. *Brain Res.* 1997;744:227-234.

Hönack D, Löscher W., Sex differences in NMDA receptor mediated responses in rats. *Brain Res.* 1993;620:167-170.

Horn, J., Haley, R. W., Kurt, T. L., Neuropsychological correlates of Gulf War Syndrome. *Arch. Clin. Neuropsychol.* 1997;12:531-544.

Ikonomidou, C., Bittigau, P., Ishimaru, M.J., Wozniak, D.F., Koch, C., Genz, K., Price, M.T., Stefovska, V., Horster, F., Tenkova, T., Dikranian, K., Olney, J.W., Ethanol-Induced apoptotic neurodegeneration and fetal alcohol syndrome, Science 2000;287:1056-1060.

Joseph, S., A Comprehensive clinical evaluation of 20,000 Persian Gulf War Veterans, *Military Medicine*, 1997;162(3):149-155.

Koek, W. and Colpaert, F.C., Selective blockade of N-methyl-D-aspartate (NMDA)-induced convulsions by NMDA antagonists and putative glycine antagonists: relationship with phencyclidine-like behavioral effects. *J. Pharmacol. Exp. Ther.*, 1990;252:349-357.

Kornhuber, J. and Weller, M., [New therapeutic possibilities with low-affinity NMDA receptor antagonists] *Nervenarzt*. 1996;67:77-82.

Leadbeater, L., Inns, R.H., Rylands, J.M., Treatment of poisoning by soman. *Fund. Appl. Toxicol.* 1985;5:S225-S231.

Löscher W, Hönack D. The novel, competitive N-methyl-D-aspartate (NMDA) antagonist CGP 37849 preferentially induces phencyclidine-like behavioral effects in kindled rats: attenuation by manipulation of dopamine, alpha-1 and serotonin 1A receptor., *J Pharmacol Exp Ther.* 1991; 257:1146-1153.

Lovinger, D.M., White, G., Weight, F.F., Ethanol inhibits NMDA-activated ion current in hippocampal neurons. Science, 243 (1989)1721-1724.

Olney, J.W., Neurotoxicity of NMDA receptor antagonists: an overview. *Psychopharmacol. Bull.*, 1994;30:533-540.

Olney J.W., Labruyere J. Price M.T., Pathological changes induced in cerebrocortical neurons by phencyclidine and related drugs [see comments]. *Science.* 1989;244:1360-2.

Olney, J.W., Labruyere, J., Wang, G., Wozniak, D.F., Price, M.T., and Sesma, M.A., NMDA antagonist neurotoxicity: mechanism and prevention. *Science.* 1991;254:1515-8.

Phillippens, I.H.C..M., Wolthuis, O.L., Busker, R.W., Langenberg, J.P., Melchers, B.P.C., Side effects of physostigmine as a pretreatment in guinea pigs. *Pharmacol. Biochem. Behav.* 1996;55:99-105.

Rothman S.M. and Olney J.W., Excitotoxicity and the NMDA receptor--still lethal after eight years. *Trends Neurosci.*. 1995;18:57-58.

Schmued, L.C., Albertson, C., Slikker, W. Jr., Fluoro-Jade: a novel fluorochrome for the sensitive and reliable histochemical localization of neuronal degeneraion. *Brain Res.* 1997;751:37-46.

Schmued, L.C. and Hopkins, K.J., Fluoro-Jade: Novel fluorochromes for detecting toxicant-induced neuronal degneration. *Toxicological Pathol.* 2000;28:91-99.

Sharp, F.R., Butman, M., Wang, S., Koistinaho, J., Graham, S.H., Sagar, S.M., Berger, P., and Longo, F.M., Heat shock proteins used to show that haloperidol prevents neuronal injury produced by ketaimine, MK801, and phencyclidine. Ann. N.Y. Acad. Sci.,1993;679:288-290.

Sharp FR., Butman M., Aardalen K. , Nickolenko J., Nakki R. , Massa SM. , Swanson RA., and Sagar SM., Neuronal injury produced by NMDA antagonists can be detected using heat shock proteins and can be blocked with antipsychotics. Psychopharmacology Bulletin. 1994**a**;30:555-60.

Taylor, P. (1998) Development of acetylcholinesterase inhibitors in the therapy of Alzheimer's disease. *Neurology*, 51(Suppl 1):S30-S35.

Tomitaka, S., Hashimoto, K., Narita, N., Sakamoto, A.,Minabe, Y. and Tamura, A., Memantine induces heat shock protein HSP70 in the posterior cingulate cortex, retrosplenial cortex and dentate gyrus of rat brain. Brain Res. 1996;740:1-5.

Vogt, B.A., Finch, D.M., and Olson, C.R., Functional heterogeneity in cingulate cortex: the anterior executive and posterior evaluative regions. *Cerebral Cortex* 1992;2:435-443.

Key Research Accomplishments

1. Blockade of N-methyl-D-aspartate (NMDA) receptors can cause neurodegeneration in certain areas of the brain. It has been hypothesized that a decrease in the excitatory drive to interneurons caused by NMDA antagonists could result in disinhibition to the principal cells and, in turn, this disinhibition (resulting in hyperexcitability) might be responsible for neurotoxicity or neuronal degeneration. We have shown that this hypothesis can be tested *in vitro*.

2. We examined the effects of the NMDA receptor antagonist, MK-801, on $GABA_A$-mediated inhibitory post-synaptic currents (IPSCs) of pyramidal neurons in the retorsplenial cortex (RSC), an area showing great sensitivity to MK-801-induced neuronal death. Using whole-cell patch clamp techniques, bicuculline-sensitive IPSCs were isolated and recorded from biocytin-labeled pyramidal neurons in the RSC and parietal cortex (Par) of rats (P14-25). Morphology of pyramidal cells filled with biocytin revealed that pyramidal cells recorded in all layers send a long apical dendrite toward the pia. In addition, these pyramidal cells also have a massive axonal arborization.

4. At holding potentials of -5 to +30 mV, bath application of MK-801 (10-40μM) caused a concentration-dependent decrease in frequency of spontaneous IPSCs in the majority of recorded pyramidal cells; MK-801 also reduced the amplitude of evoked $GABA_A$ receptor-mediated IPSCs in pyramidal neurons recorded in layer II-VI.

5. When compared to pyramidal neurons in the parietal cortex, MK-801 showed a greater inhibitory effect on IPSCs in the RSC.

6. In the presence of 0.5 μM tetrodotoxin (TTX), the amplitude and frequency of the mini-nature IPSCs (mIPSCs) were not affected by bath application of MK-801 (40 μM), indicating that MK-801 exerts its inhibitory effect on IPSCs through an action potential dependent mechanism.

7. Taken together, the results from patch-clamp recording suggest that NMDA receptors regulate GABA release, and blockade of NMDA receptors causes a region-specific decrease in inhibitory synaptic transmission to pyramidal cell. This effect may be via presynaptic mechanisms that may suppress excitatory drive to inhibitory interneurons and therefore could promote region-specific neurotoxicity.

8. Fluoro-Jade staining shows that MK-801 (0.3-3 mg/kg) alone causes dose-dependent neurodegeneration in the posterior cingulate gyrus or retrosplenial cortex in adult female rats. This is seen 3 days after a single s.c. injection of MK-801, suggesting that more degeneration than previously though occurs after a single low dose of MK-801.

9. Fluoro-Jade staining shows that pyridostigmine bromide PB (0.1 mg/kg) alone does not cause

neurodegeneration in the posterior cingulate gyrus or retrosplenial cortex. In addition, at this low dose of PB, there does not appear to be any gross enhancement of low-dose (3μM) MK-801-induced neurodegeneration. In selected animals, PB may be slightly protective, more studies must be done to carefully evaluate this preliminary result.

10. Photodiode images of voltage-sensitive dye-treated slices show brain slices from adult female rats can survive in our *in vitro* system and will be useful to explore neurotoxic mechanism of NMDA antagonists and the effect of co-exposure to AChE inhibitors.

11. Photodiode imaging shows that in cingulate/retrosplenial cortical slices from adult female rats, MK-801 (3 μM) enhances evoked depolarizations.

12. Photodiode imaging shows that in cingulate/retrosplenial cortical slices from adult female and young male rats, pyridostigmine bromide (100 μM) inhibits evoked depolarizations.

Reportable Outcomes:

Abstracts:*

The following two abstracts are for presentations at the Society for Neuroscience Annual Meeting (Nov. 4-9th, 2000).

1. MK-801, an NMDA Receptor Antagonist, Modulates the inhibitory postsynaptic currents (IPSCs) in Pyramidal Neurons in the Cingulate Cortex of Rats. Q. Li, S. Clark, W.A.Wilson, D.V. Lewis.

2. Effects of N-methyl-D-aspartate (NMDA) Antagonists & Acetylcholinesterase Inhibitors (AChEIs): Fluoro-Jade Staining, Behavior, & Photodiode Array Imaging. S. Clark, Y. D. Phillips, C. Wang, A. K. Shetty, V. Zaman, K. H. Jones, W.A. Wilson.

*Copies of the abstracts are provided in the Appendicies.

Conclusions:

At the end of one year of work, we are pleased to have shown that we can use sophisticated electrophysiology, voltage-sensitive dye imaging, and state-of-the-art neurohistology to study the effects of NMDA antagonists and anticholinesterase agents on discrete brain areas.

As described above, our first-year work shows that NMDA antagonists do suppress synaptic inhibition in principle cells of the cingulate/retrosplenial cortex gyrus. This action, seen in single cells with whole cell patch recording, is the first electrophysiological study which shows a potential basic mechanism underlying the neurotoxicity of NMDA antagonists at the single cell level.

Our use of a photodiode array to sense voltage changes in cells treated with a voltage sensitive dye has proven to be a powerful tool for studying the effects of NMDA antagonists and an anticholinesterase on cell populations in the cingulate/retrosplenial area. We showed, as expected that the NMDA antagonists produced population excitability. We were stunned to find that the anticholinesterase did not increase the excitability, but in fact, reduced it. This data is counter to our original hypothesis, but may prove very important.

Finally, we performed histological studies with the dye Fluro-Jade to look for neurotoxicity following treatment with NMDA antagonists and pyridostigmine. Again these studied confirmed that the NMDA antagonist MK-801 was toxic, but we were surprised to find that pyridostigmine did not enhance the toxicity, but perhaps suppressed it.

So what does this mean? Studies that deal with the toxic effects of NMDA antagonists in this brain area show that the toxicity is enhanced by muscarinic cholinergic agents and suppressed by muscarinic cholinergic antagonists. So, how could pyridostigmine be protective? Two explanations seem possible. First, pyridostigmine might have properties that have nothing to do with suppression of cholinesterase activity. Second, pyridostigmine might be raising the level of acetylcholine at nicotinic receptors and thus providing neuroprotection.

We believe that this surprising effect of pyridostigmine must be addressed in our second year of research. We will examine other anticholinesterase agents and we will treat slices with nicotinic antagonists. These experiments will give us clues to the origin of the pyridostigmine protective effect.

In summary, we feel we have made great progress in setting up the systems to carry out electrophysiology, imaging, and histology. Moreover we have achieved successful and publishable experiments with greater speed than we could have reasonably expected. Best of all, we have results that suggest a path toward understanding why pyridostigmine might be neuroprotective and how to develop more effective neuroprotective strategies.

References:

A list of complete references are included at the end of every study.

Appendices:

Two abstracts and one manuscript are attached.

Abstract View

MK-801, A NMDA RECEPTOR ANTAGONIST, MODULATES THE INHIBITORY POSTSYNAPTIC CURRENTS (IPSCS) IN PYRAMIDAL NEURONS IN THE CINGULATE CORTEX OF RATS.

Q. Li*; S. Clark; W. Wilson; D.V. Lewis

Dept. of Ped.Neurology., Pharmacol. and Can. Bio., DUMC and Neurology Research, VAMC., Durham, NC,

N-methyl-D-aspartate (NMDA) antagonists can be neurotoxic and the most sensitive areas are the posterior cingulate (PS) and the retrosplenial cortex (RSC)(Olney et al, 1991). Anatomical evidence suggests that the toxic mechanism may be a complex, disinhibitory process, but no direct electrophysiological evidence exists. We report here such evidence. We examined the effects of MK-801, a NMDA receptor antagonist, on the $GABA_A$-mediated IPSCs of pyramidal neurons in the RSC. Using whole-cell patch clamp techniques, bicuculine-sensitive IPSCs were isolated and recorded from biocytin-labeled pyramidal neurons in the RSC and parietal cortex (Par) of rats (P14-P25). At the holding potential of +30 mV, outward post-synaptic currents were observed. Bath application of MK-801 (10-40μM) caused a dose-dependent decrease in frequency of spontaneous $GABA_A$ IPSCs in 85% of recorded neurons; the amplitude of evoked $GABA_A$ IPSCs was also reduced by MK-801. However, MK-801 showed a much less inhibitory effect on $GABA_A$ IPSCs of pyramidal neurons in the Par. With 0.5μM tetrodotoxin (TTX), the amplitude and frequency of the miniature IPSCs were not significantly affected by MK-801 (40μM). These results suggest that NMDA receptor blockade causes a decrease in inhibitory synaptic transmission to pyramidal neurons; this effect may be due to suppression of excitatory drive to the inhibitory interneurons and could therefore promote neurotoxicity.

Supported by: DOD (DAMA17-99-1-9541) and NIH (DA-06735) grants.

close

Abstract View

EFFECTS OF *N*-METHYL-D-ASPARTATE ANTAGONISTS AND ACETYLCHOLINESTERASE INHIBITORS: FLUORO-JADE STAINING, BEHAVIOR, AND PHOTODIODE ARRAY IMAGING.

S. Clark*; Y.D. Phillips; C. Wang; A.K. Shetty; V. Zaman; W.A. Wilson

VA Neurol, Research & Duke Depts. Pharmacol. & Cancer, Biol. & Neurosurg. Veterans Admin. Med Cntr., Durham, NC, USA

NMDA antagonists (e.g. MK-801 & phencyclidine) produce neurotoxicity in the posterior cingulate (PC) & retrosplenial gyrus (RSG) (Olney *et al.* '89). This is exacerbated by the cholinergic agonist pilocarpine (Corsco, *et al.* '97). Do AChEIs exacerbate this neurotoxicity? Such an interaction may have clinical, environmental, and military importance.

This interaction was studied using behavioral monitoring and Fluoro-Jade (F-J) (a fluorochrome that detects degenerating neurons- including injury by NMDA antagonists (Schmued & Hopkins,'00)). Adult female rats were treated with MK-801 (0.3-3mg/kg) ± physostigmine (1mg/kg) or pyridostigmine (0.1mg/kg), monitored 3 hours, allowed to recover for 3 days, perfusion-fixed, and cryostat-sectioned (40 μm). In the PC/RSG, dose-dependent positive F-J staining was seen after MK-801 alone. Alone, AChEIs did not cause positive F-J staining and AChEIs had no effect on toxicity of high-dose MK-801. However, pyridostigmine reduced toxicity of low-dose (0.3) MK-801 (ave. F-J +cells per PC/RSG region/section: 21.7 (MK-801) *vs.* 2.2 (MK-801+pyridostigmine). Results of behavioral tests paralleled histopathology. Neurotoxic mechanisms were explored *in vitro* in PC/RSG slices using a photodiode array and voltage-sensitive dye to monitor evoked activity. In slices with PC/RSG, evoked depolarizations were enhanced by bath-applied MK-801 (10μM); AChEIs did not increase this. Thus, AChEIs have more complex interactions with NMDA antagonists than direct cholinergic agonists such as pilocarpine (but by as-yet unknown mechanisms). DAMD17-99-1-9541; Durham VAMC IMR-Clark01; NIH-NS36741.

close